C.3

LA-3204-MS

LOS ALAMOS SCIENTIFIC LABORATORY
OF THE UNIVERSITY OF CALIFORNIA o LOS ALAMOS NEW MEXICO

CALCULATION OF RETINAL DOSE DUE TO VISIBLE RADIATION FROM NUCLEAR EXPLOSIONS

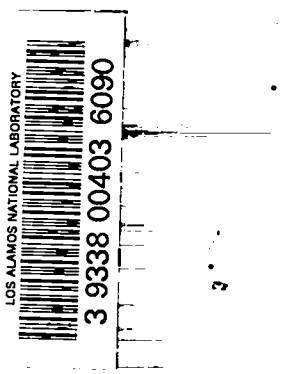

LEGAL NOTICE

Printed in USA. Price $ 4.00. Available from the

Clearinghouse for Federal Scientific
and Technical Information,
National Bureau of Standards,
U. S. Department of Commerce,
Springfield, Virginia

LA-3204-MS
UC-41, HEALTH AND SAFETY
TID-4500 (36th Ed.)

LOS ALAMOS SCIENTIFIC LABORATORY
OF THE UNIVERSITY OF CALIFORNIA LOS ALAMOS NEW MEXICO

REPORT WRITTEN: October 6, 1964

REPORT DISTRIBUTED: March 1, 1965

CALCULATION OF RETINAL DOSE DUE TO VISIBLE RADIATION FROM NUCLEAR EXPLOSIONS

by

Robert D. Cowan

Contract W-7405-ENG. 36 with the U. S. Atomic Energy Commission

Abstract

Calculation of the maximum energy density received by any portion of the retina due to radiation from an incompletely resolved source requires knowledge of the point-source retinal-image-spread function. For a uniform circular source, one requires more specifically: (1) the point-source effective image radius a_o, and (2) the normalized integral $g(a/a_o)$ of the image spread function out to the geometrical image radius a. The function g tends to a^2/a_o^2 for small a, to unity for large a, and in intermediate regions may be roughly characterized by its value at $a = a_o$. Experimental measurements on human eyes appear to indicate $a_o > 6$ microns and $g(1) \cong 0.5$, but these values are uncertain. A theoretical calculation assuming only diffraction and chromatic aberration gives $a_o = 3.5\mu$ and $g(1) \cong 0.15$ for large pupils (nighttime conditions) and $a_o = 4\mu$, $g(1) \cong 0.4$ for small pupils (daytime). Less conservative results, in which effects of other aberrations have been incorporated, are $a_o \cong 7\mu$, $g(1) \cong 0.5$ for any size pupil -- in reasonable agreement with experiment. The dose from a hypothetical high-altitude explosion is calculated to illustrate use of these results.

Table of Contents

Page

Abstract 3

Sec. 1. Introduction 9

Sec. 2. Calculation of Retinal Dose 11

Sec. 3. Experimental I(r) and a_o 16

Sec. 4. Theoretical I(r) and a_o 25

A. Model of the Eye 25

B. I(r) and a_o for Diffraction Only 33

C. Chromatic Aberration of the Eye 37

D. I(r) and a_o for Diffraction Plus Chromatic Aberration . . . 45

E. Effects of Age and Individual Variations 61

F. Other Aberrations 69

Sec. 5. Summary and Conclusions 75

Sec. 6. Example 84

Appendix 93

References 98

Figures

Fig. 1. Hypothetical Forms of Image-Spread Function 18

Fig. 2. Correction Function $g = I(o)/I_{geom}$ 19
Fig. 3. Schematic Eye 29
Fig. 4. Entrance Pupil 29
Fig. 5. Exit Pupil 29
Fig. 6. Schematic Eye 31
Fig. 7. Reduced Eye 31
Fig. 8. Simplified Reduced Eye 31
Fig. 9. Image-Spread Function for Diffraction Only 35
Fig. 10. Correction Function g for Diffraction Only 36
Fig. 11. Transmission of Human Eye 38
Fig. 12. Chromatic Aberration of the Human Eye 41
Fig. 13. Out-of-Focus Diffraction Patterns 49
Fig. 14. Image-Spread Function for Diffraction plus Chromatic Aberration 58
Fig. 15. Correction Function g for Diffraction plus Chromatic Aberration 59
Fig. 16. Reduced Eye with Spectacle Lens 65
Fig. 17. Meridional Rays for Spherical Interface 71
Fig. 18. Intensity Averaged over Circle of Radius r_o 74
Fig. 19. Renormalized Average Intensity 76
Fig. 20. g for Averaged Intensity 77
Fig. 21. Upper and Lower Limits of g(x) 83
Fig. 22. Radius, Temperature, and Brightness History of Hypothetical High-Altitude Explosion 86

Fig. 23. Instantaneous Peak Retinal Intensity and Integrated Peak Retinal Dose for g_1 87

Fig. 24. Integrated Peak Retinal Dose from Hypothetical High-Altitude Explosion 89

Fig. 25. Threshold Dose for Retinal Burns in Rabbits 91

Fig. A-1. Schematic Eye with Supplementary Lens 95

Tables

Table I. Gullstrand's Schematic Eye 27

Table II. Transmission of Water and the Human Eye, and Dispersion of Water 39

Table III. Values of a_o from Machine Calculation, Diffraction Plus Chromatic Aberration 57

Table IV. Values of a_o and g(1) for I_{ave} 79

1. Introduction

Due to the very high brightnesses involved, the thermal radiation from high-altitude nuclear explosions may produce serious burns on the retina of persons viewing such explosions. This hazard is of special importance since the burst may be visible above the horizon to casual observers 1000 or more kilometers from ground zero.

Assuming the brightness-radius-time history of the source to be known, the calculation of the thermal dose on the retina is a straightforward and fairly simple problem when the retinal image is fully resolved, being then a problem in geometrical optics involving (besides the question of atmospheric and intra-ocular transmission) only the well-known geometry of the human eye. When the image is incompletely resolved the problem is much more complicated, involving not only diffraction effects but also various chromatic and geometrical aberrations of which we have rather inadequate quantitative knowledge. (Brief surveys and extensive bibliographies regarding ocular aberrations may be found in papers by Westheimer[1] and Fry.[2])

There exist in the report literature a number of attempts to treat the retinal-dose problem. Most of these are of limited interest, either dealing only with the fully-resolved case, or treating the point-source

case in only a rough approximation. We mention here only the work of Mayer, et al.,[3] who give a detailed treatment of chromatic aberration, but account only approximately for the equally important effects of diffraction (ultimately tying their conclusions to experimental results of uncertain validity), and do not explicitly discuss the case of a partially resolved source (though they calculate the necessary integral of the point-source image-spread function).

In the present paper, we derive in Sec. 2 the necessary equations for calculating the retinal dose, for an arbitrary size of the geometrical retinal image. Ultimately these of course require knowledge of the point-source image-spread function $I(r)$, but it is shown that everything can be conveniently expressed in terms of an effective point-source image radius a_o and a function $g = g(a/a_o)$ of the ratio of geometrical image radius to a_o. In Sec. 3, an attempt is made to obtain the function $I(r)$ -- and hence also a_o and g -- from direct experimental measurements on human eyes. Since the interpretations of the experimental data are uncertain, a theoretical calculation is made in Sec. 4 -- consisting of an idealized but honest calculation of diffraction effects, combined with a treatment of chromatic aberration similar to that of Mayer, et al.* Since spherical and other aberrations are neglected, the result should provide a conservative (over-) estimate of the retinal dose. The effects

---

*The calculation is identical in principle with one by Fry,[4] whose work was unknown to the author till after this report was written. The present report gives the calculation in greater detail, along with more extensive numerical results.

of optical aberrations and scattering within the eye and retina are estimated semi-quantitatively, giving results which are less conservative but probably more realistic (and apparently in better agreement with the above-mentioned experiments). The entire calculation and its results are summarized in Sec. 5 for those not interested in the details of Secs. 2-4. Finally, in Sec. 6 the detailed calculation of retinal dose is outlined for a hypothetical (but realistic) explosion in vacuum, with a yield of about a megaton.

2. Calculation of Retinal Dose

Assuming a spherically-symmetric opaque source of radius R, the apparent brightness is uniform over the entire disk of area πR^2. This brightness B, measured in watts/cm^2-ster, corresponds to the rate of radiation of energy in a "visible" spectrum to be defined more precisely later on.* If T is the suitably weighted average transmission of the atmosphere and eye along the path from source to retina then the power passing through the entrance pupil of radius r_p at a distance D from the source is

$$T \cdot B \cdot \pi R^2 \cdot (\pi r_p^2/D^2) \quad \text{watts} .$$

*Strictly speaking, the quantity B is not a brightness at all (having nothing whatever to do with the photosensitivity of the eye), but is rather the radiance of the source in the "visible" region. However, we shall stick to this misnomer, which is in common local use.

If the eye produced a perfect geometrical image of a size corresponding to a focal length f_o, the retina would be uniformly illuminated over a circular area of radius

$$a = R\, f_o/D \tag{1}$$

with an intensity

$$I_{geom} = \frac{\pi^2 T\, B\, R^2 r_p^2}{D^2 \cdot \pi\, a^2} = \frac{\pi\, T\, B\, r_p^2}{f_o^2} \quad \text{watts/cm}^2 \,. \tag{2}$$

For a sufficiently large source, giving a more-or-less-completely resolved image on the retina, this will be the value of the actual intensity on the retina (except near the edges of the image). For small sources, however, diffraction effects and optical imperfections in the eye cause the energy falling on the retina to be spread over an area much larger than $\pi\, a^2$; consequently, the peak intensity in the retinal image is smaller than the geometrical value (2). We now calculate the appropriate correction factor.

To be as conservative as possible, we assume the eye to be perfectly stigmatic. Then for a very small source corresponding to a geometrical retinal image of infinitesimal area dA, the actual intensity distribution on the retina may be assumed to be given by

$$I(r)dA \,, \tag{3}$$

where $I(r)$ is some radially symmetric function which we assume to have a maximum value at $r = 0$ and to decrease more or less monotonically with increasing r. For a finite source corresponding to a uniform geometrical retinal image of radius a, the actual image will then have a maximum intensity at the center, and this intensity will be given by integrating $I(r)$ over all those values of r which pile up at the center of the actual image due to the finite radius a of the geometrical image:

$$I_{max} = \int I(r)(dA)_{geom} = \int_0^a I(r)2\pi\, r\, dr\ , \qquad (4)$$

where r is the distance from the element dA of the geometrical image to the center of the actual image. Now the total power falling on the retina from the infinitesimal source is from (3)

$$dA \int_0^\infty I(r)2\pi\, r\, dr\ ,$$

so that for the finite source it is

$$\pi\, a^2 \int_0^\infty I(r)2\pi\, r\, dr\ .$$

By definition of I_{geom}, this last value must be equal to $I_{geom}\pi\, a^2$, so that

$$I_{geom} = \int_0^\infty I(r) 2\pi\, r\, dr \,. \qquad (5)$$

(This result can of course also be obtained from (4) by noting that I_{geom} must be the maximum value which I_{max} can build up to as the source size is increased.) The required correction factor for an incompletely resolved image is thus

$$g \equiv \frac{I_{max}}{I_{geom}} = \frac{\int_0^a I(r) r\, dr}{\int_0^\infty I(r) r\, dr} \,. \qquad (6)$$

In terms of this function, the integrated maximum retinal dose is from (2)

$$\text{Retinal dose} \equiv \int I_{max}\, dt$$

$$= \int g\, I_{geom}\, dt$$

$$= \frac{\pi\, T\, r_p^2}{f_o^2} \int g\, B\, dt \qquad \text{joules/cm}^2$$

$$= \frac{\pi\, T\, r_p^2}{4.18\, f_o^2} \int g\, B\, dt \qquad \text{cal/cm}^2 \,, \qquad (7)$$

where the integral is to be evaluated over an interval equal to the reflex blink period of the eye (about 0.15 sec). Thus evaluation of the retinal dose requires only a knowledge of the normalized integral g(a) of the point-source image-spread function out to the radius a of the geometrical image. Before looking into the problem in detail, we can make a few semiquantitative comments regarding the form of g(a):

It is convenient to introduce an effective radius a_o of the point-source image-spread function I(r) such that a geometrical image of uniform intensity I(o) having this radius would contain the same total power as the actual point-source image:

$$\pi\, a_o^2 I(o) \equiv \int_o^\infty I(r) 2\pi\, r\, dr\ . \tag{8}$$

In terms of a_o,

$$g = \frac{\int_o^a I(r) r\, dr}{a_o^2 I(o)/2}\ . \tag{9}$$

In the limit of small a, this clearly tends to the proper value

$$g_{a\to o} = \frac{a^2}{a_o^2} = \frac{\text{geometrical area}}{\text{point-source effective area}}\ . \tag{10}$$

For larger values of a, the effective area is larger than the point-

source value, so that the value of g decreases more and more below the limiting value (10), and g of course gradually tends to the opposite limit

$$g_{a\to\infty} = 1 \ , \tag{11}$$

from (6). In the intermediate range where a is comparable to a_o, a reasonable estimate for the effective area is $\pi(a_o^2 + a^2)$, and we then have the expression

$$g \cong \frac{a^2}{a_o^2 + a^2} = \frac{a^2/a_o^2}{1 + a^2/a_o^2} \ , \tag{12}$$

which shows the proper limiting behavior (10) and (11), and should be roughly correct for all values of a.

In general, it will be convenient to think of g as a function $g(a/a_o)$ of the reduced variable a/a_o. We shall calculate more refined forms of this function, but since (12) is already reasonably accurate, our main problem is to arrive at an appropriate value of a_o.

3. Experimental I(r) and a_o

We first attempt to deduce I(r), $g(a/a_o)$, and a_o from the results of several recent experimental investigations.[5-9] [From now on we shall usually consider I(r) normalized to the value I(o) = 1.]

(a) References 5, 7, and 8 suggest that for a narrow <u>line</u> source,

I is approximately a simple exponential function of the distance from the middle of the retinal image. For a point source, the form of I(r) would be somewhat different, but not greatly so. If we then assume an exact exponential, we have

$$I(r) = e^{-(\ell n\ 2)r/r_h} , \tag{13}$$

where r_h is the half width at half maximum. A simple integration gives

$$\int_0^a I(r)r\ dr = \left(\frac{r_h}{\ell n\ 2}\right)^2 \left[1 - \left(1 + \frac{a\ \ell n\ 2}{r_h}\right) e^{-(a\ \ell n\ 2)/r_h}\right] , \tag{14}$$

from which

$$\int_0^\infty I(r)r\ dr = (r_h/\ell n\ 2)^2 . \tag{15}$$

Thus for the distribution (13) we find from (8) and (6):

$$a_o = \sqrt{2}\ r_h/\ell n\ 2 = 2.04 r_h , \tag{16}$$

$$g(a/a_o) = 1 - [1 + \sqrt{2}(a/a_o)]e^{-\sqrt{2}(a/a_o)} . \tag{17}$$

The functions (13) and (17) are plotted in Figs. 1 and 2, respectively. Note that (13) has appreciable magnitude to quite large values of r/r_h,

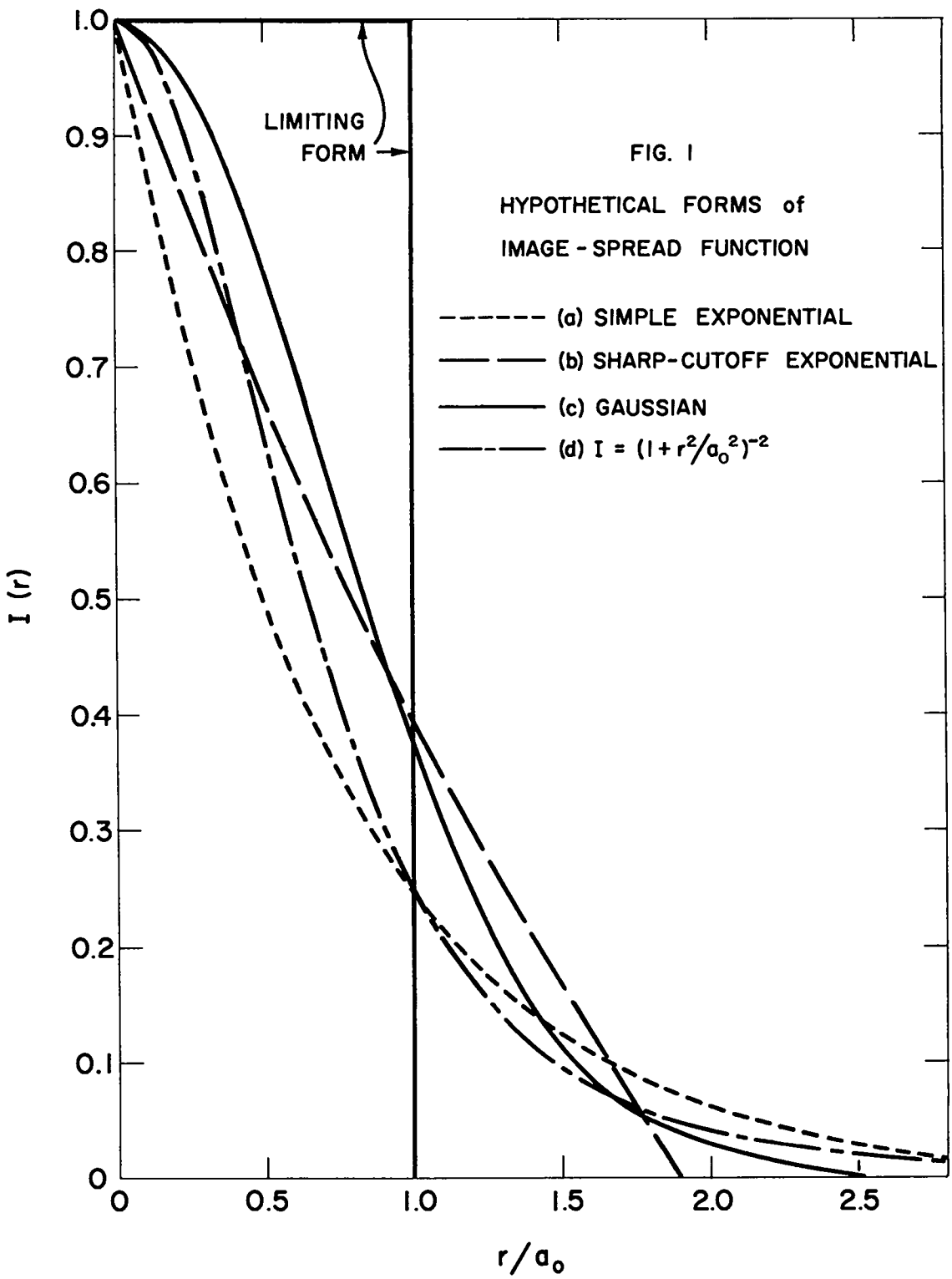
1.0
0.9
0.8
0.7
0.6
0.5
0.4
0.3
0.2
0.1
0
I (r)
0
0.5
1.0
1.5
2.0
2.5
r/a₀
LIMITING FORM
FIG. 1
HYPOTHETICAL FORMS of IMAGE - SPREAD FUNCTION
(a) SIMPLE EXPONENTIAL
(b) SHARP-CUTOFF EXPONENTIAL
(c) GAUSSIAN
(d) I = (1 + r²/a₀²)⁻²

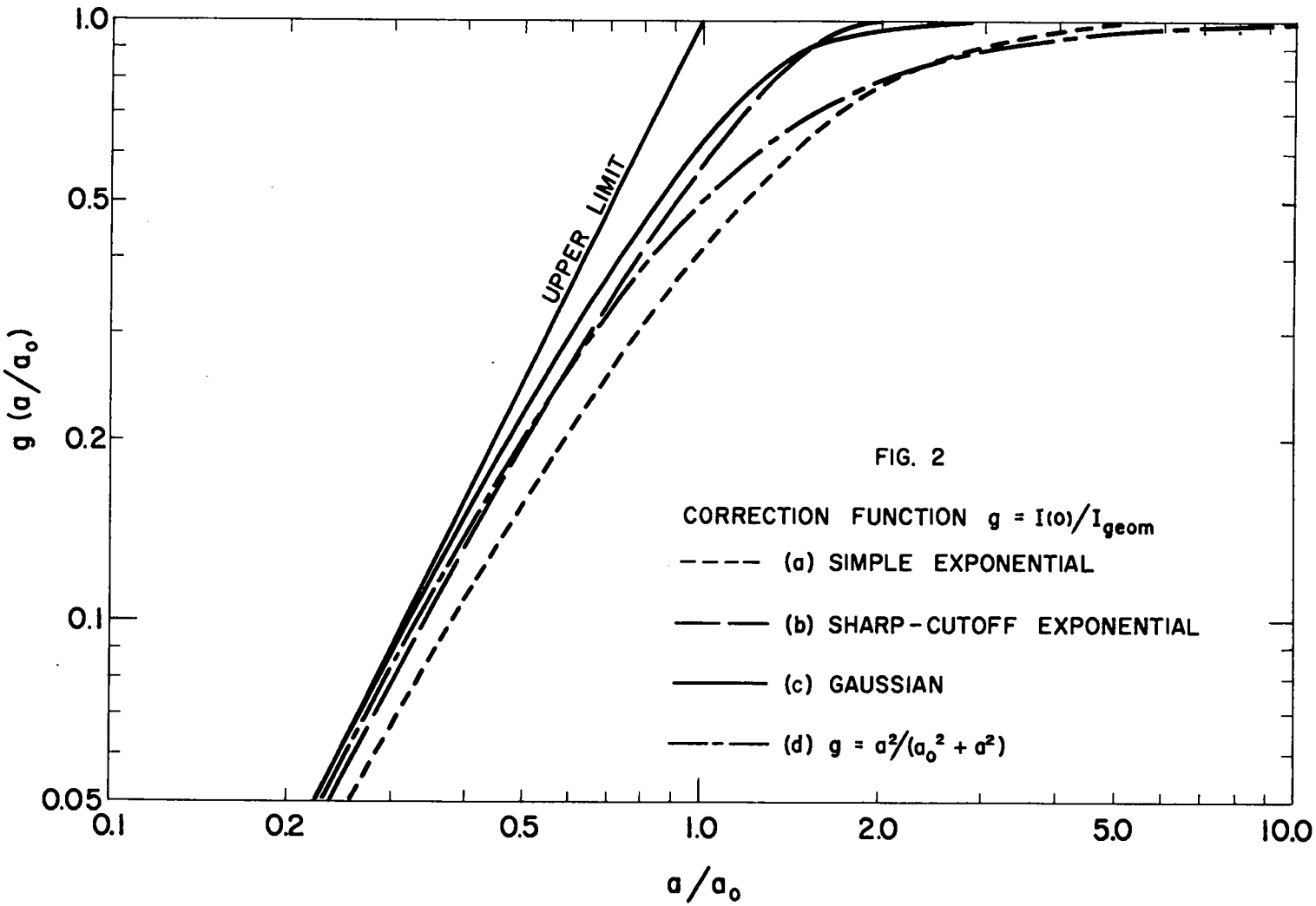

FIG. 2

CORRECTION FUNCTION $g = I(0)/I_{geom}$

---- (a) SIMPLE EXPONENTIAL

—— (b) SHARP-CUTOFF EXPONENTIAL

——— (c) GAUSSIAN

—·— (d) $g = a^2/(a_0^2 + a^2)$

thereby resulting in the rather large ratio $a_o/r_h = 2.04$.

(b) For a conservative calculation of eye dose it seems preferable to consider a function I(r) which cuts off more sharply than does (13). Such a function may indeed be deduced from the results of reference 6: Ogle used two "point" sources of variable intensity and variable separation. For each separation he varied their intensity so as to determine the visible threshold. The threshold source-intensity level was found to vary exponentially with the separation up to a (geometrical) separation a_{max} on the retina, beyond which the intensity level did not have to be increased further. If we assume each source to produce an intensity distribution I(r) on the retina for unit source intensity, and assume the threshold intensity to be equal to the total (peak) intensity at the center of the image of either of the two sources, then Ogle's results imply

$$e^{cr}[I(o) + I(r)] = \text{constant} , \qquad r \leq a_{max} .$$

Taking as usual I(o) = 1 and assuming I(r) = 0 for $r > a_{max}$, then

$$I(r) = K\, e^{-cr} - 1 = 2e^{-(\ln 4/3)r/r_h} - 1 \tag{18}$$

for

$$0 \leq r \leq a_{max} = \frac{\ln 2}{\ln 4/3}\, r_h = 2.410 r_h . \tag{19}$$

Integration of (18) gives

$$a_o = 1.269 r_h \ , \tag{20}$$

$$g \equiv \int_o^a I\, r\, dr \Big/ \int_o^{a_{max}} I\, r\, dr$$

$$= 30.02[1 - (1 + z)e^{-z} - z^2/4] \ , \qquad a \leqq a_{max} = 1.90 a_o \ , \tag{21}$$

where

$$z = 0.3650 a/a_o \ . \tag{22}$$

The functions (18) and (21) are also shown in Figs. 1 and 2. As anticipated, the sharp cutoff of (18) causes (21) to rise to unity considerably faster than does (17), and also results in a much smaller value of a_o/r_h than (16).

(c) Inasmuch as the experimental bases of both (13) and (18) are open to numerous objections, and in any case we should not expect I(r) to show a cusp at r = 0, we also make a calculation for a hypothetical Gaussian distribution,

$$I(r) = e^{-(\ell n\ 2)(r/r_h)^2} \ . \tag{23}$$

Then

$$\int_o^a I(r) r\, dr = \frac{r_h^2}{2\ \ell n\ 2}\left[1 - e^{-(\ell n\ 2)(a/r_h)^2}\right], \tag{24}$$

$$a_o = r_h/\sqrt{\ln 2} = 1.201 r_h \ , \tag{25}$$

$$g = 1 - e^{-(a/a_o)^2} \ . \tag{26}$$

(d) The form of I(r) which corresponds to the approximate g function (12),

$$g = \frac{a^2}{a_o^2 + a^2} \ , \tag{27}$$

is easily found by differentiating (9):

$$\int_0^a I(r) r \, dr = \frac{a^2 a_o^2/2}{a_o^2 + a^2}$$

$$I(a) \cdot a = \frac{(a_o^2 + a^2) a \, a_o^2 - a^3 a_o^2}{(a_o^2 + a^2)^2}$$

$$I(r) = \frac{a_o^4}{(a_o^2 + r^2)^2} \ , \tag{28}$$

from which

$$a_o = (\sqrt{2} - 1)^{-1/2} r_h = 1.554 r_h \ . \tag{29}$$

(e) An absolute upper limit to g and an absolute lower limit to a_o/r_h is given by the rectangular function

$$I(r) = \begin{cases} 1 , & a \leq a_o , \\ 0 , & a > a_o . \end{cases} \tag{30}$$

Then

$$a_o = r_h , \tag{31}$$

and

$$g = \begin{cases} a^2/a_o^2 , & a \leq a_o , \\ 1 , & a > a_o . \end{cases} \tag{32}$$

The various image spread functions $I(r)$ assumed above are shown in Fig. 1, and the corresponding functions $g(a/a_o)$ are shown in Fig. 2. It may be seen from the latter figure that there is not too much ambiguity in the function g; it would seem unlikely that the rough form (12) or (27), for example, is incorrect by more than about 30 percent at any value of a.

However, a value of a_o is most easily deduced from experimental values of the half-width r_h; and since values derived above for a_o/r_h run all the way from 1 to 2.04, there is considerable ambiguity in the implied value of a_o. From (7) and (10), the calculated retinal dose for small sources is inversely proportional to a_o; hence a conservative

estimate of dose requires use of a reasonably small value of a_o -- perhaps $a_o = 1.3r_h$.

For thin line sources (half-width 0.25 to 0.8′), the half-width r_h has been measured experimentally[5,7,8] at about one minute of arc for a 3mm diameter pupil, and at 1.3 to 2.5′ for a 6 to 8mm pupil. Since we are interested in large pupil diameters [which from (7) will give the largest retinal dose], and since the value $r_h = 1.3'$ was obtained with semi-monochromatic light (thereby tending to reduce the chromatic aberration; see, however, reference 9 and Sec. 4D below), we can probably assume a value 1.5′ for our purposes. It is estimated[7,10] that a point-source function would have a half-width only two-thirds that for a line source; hence for the former we obtain $r_h = 1.0'$. Using point-sources directly, the cutoff value a_{max}, Eq. (19), was measured[8] at 2.6 to 4′ for 4 to 4.8mm pupils; assuming the line shape (18), this implies from (19) that $r_h = 1.1$ to 1.7′. Since this is for relatively small pupils, then even allowing for a source radius of 0.3′ we can again assume $r_h = 1.0'$. With a focal length of about 17mm for the eye, we then find

$$a_o \cong 1.3r_h \cong 1.3' = 0.00038 \text{ radians}$$

$$= 6.4 \text{ microns} . \qquad (33)$$

A straightforward, somewhat uncritical interpretation of the experiments thus indicates a value of about 6μ to be a reasonable value to use for the effective image radius of a point source. However, the

possibilities for error introduced by finite source size and in both execution and interpretation of the experiments are numerous. Moreover, the experiments were performed on a very limited number of individuals, and it is unknown to what extent other individuals might have significantly better vision than indicated by the value $a_o = 6\mu$. For these reasons, it seems desirable to make a theoretical calculation of the minimum reasonable value to be expected for a_o.

4. Theoretical I(r) and a_o

A. Model of the Eye

In order to make theoretical calculations, it is necessary to choose a model of the eye which is a good approximation to the average adult human eye. Many such schematic eyes have been proposed, differing from each other in minor details; we shall use that defined in Table I, as modified slightly in Fig. 3, which is drawn for zero accommodation (focussed at infinity).[11,12] Ignoring aberrations, the focal points FF′ and principal planes HH′ have the geometrical significance[13] that any light ray entering the eye along a path parallel to the optic axis passes through F′, travelling through the vitreous humor in the same direction as though the entire refraction of the ray occurred at H′; likewise, a ray travelling through the vitreous humor in an anterior direction parallel to the axis leaves the cornea along a path through F as though the entire refraction occurred at H. The nodal points NN′ are such that

any ray entering the eye along an external path aimed toward N will travel through the vitreous humor along a parallel path passing through N′. The distances $\overline{FH}$ and $\overline{N'F'}$ are equal, as are $\overline{HH'}$ and $\overline{NN'}$. The distance $\overline{H'F'}$ (the posterior focal length f′) is equal to the index of refraction of the vitreous humor (n′) times the anterior focal length $f = \overline{FH}$. This implies

$$n' = \frac{f'}{f} = \frac{22.8}{17.1} = \frac{4}{3} \tag{34}$$

(i.e., the vitreous humor has essentially the same index as does water). The position of the image I of some object O can be found geometrically by means of the above properties, or analytically from the relation

$$(\overline{OF}) \cdot (\overline{F'I}) = ff' \tag{35}$$

or the relation

$$\frac{f}{\overline{OH}} + \frac{f'}{\overline{H'I}} = 1 \, . \tag{36}$$

Of importance for our purposes are the entrance and exit pupils of the eye [i.e., the images of the physical pupil (the iris i of Fig. 3) as viewed from outside the eye and from the retina, respectively]; the former determines how large a pencil of light enters the eye, and the latter is required for the calculation of diffraction and chromatic aberration. The geometrical constructions for finding the locations

TABLE I

GULLSTRAND'S SCHEMATIC EYE[a]
(Accommodation Relaxed)

Indices of refraction	
Cornea	1.376
Aqueous and vitreous	1.336
Lens	1.386
Equivalent core lens	1.406

Surfaces	Position	Radius of curv.	Refracting power
Anterior surface cornea	0 mm	7.7 mm	48.83 diop
Posterior surface cornea	0.5	6.8	-5.88
Anterior surface lens	3.6	10.0	5.0
Core Lens	-	-	5.99
Posterior surface lens	7.2	-6.0	8.33
Fovea centralis	24.0		

Systems	Cornea	Lens	Complete eye
Refracting power	43.05	19.11[b]	58.64
Position of first principal point	-0.050	5.68	1.35
Position of second principal point	-0.051	5.81	1.60
Anterior focal length	23.23	69.91[c]	17.06
Posterior focal length	31.03	69.91	22.79

[a] Reference 11.

[b] For the lens in air (power in medium of n = 1.336 is 14.30).

[c] For the lens in medium of refractive index 1.336.

and sizes of these pupils are shown in Figs. 4 and 5, with cardinal points of the corneal and lens systems only taken from Table I. The corresponding algebraic calculations are, using (35) for location, and similar triangles for size:

(a) Entrance pupil

$$\overline{F'I} = \frac{31.0 \cdot 23.2}{-(31.0 - 3.4)} = -26.1 \qquad \text{(I 2.9 to right of H'H)} ,$$

$$\frac{r_n}{r_i} = \frac{7.8 - 2.9}{7.8 - 3.4} = \frac{4.9}{4.4} = 1.11 .$$

Thus the entrance pupil is 0.5mm in front of the iris and 11 percent larger.

(b) Exit pupil

$$\overline{F'I} = \frac{69.9 \cdot 69.9}{-(69.9 - 2.2)} = -72.2 \qquad \text{(I 2.3 to left of H')} ,$$

$$\frac{r_x}{r_i} = \frac{2.3}{2.2} = 1.05 .$$

Thus the exit pupil is essentially coincident with the iris except that it is five percent larger; it lies 21.2mm to the left of the retina, and is six percent smaller than the entrance pupil. The schematic eye of Fig. 3 is redrawn in Fig. 6, showing the entrance and exit pupils, and a ray entering parallel to the optic axis which passes through the boundaries of the pupils.

FIG. 3

SCHEMATIC EYE

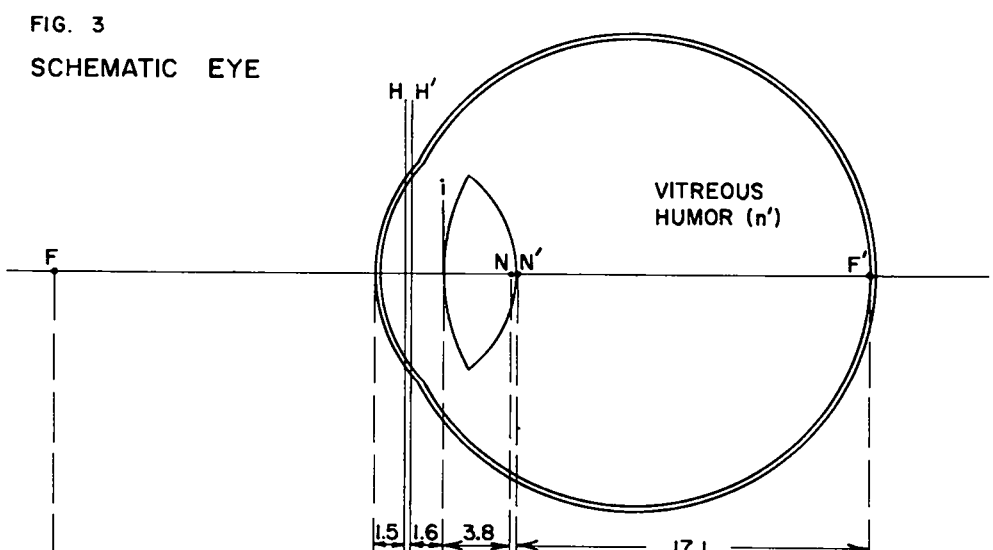

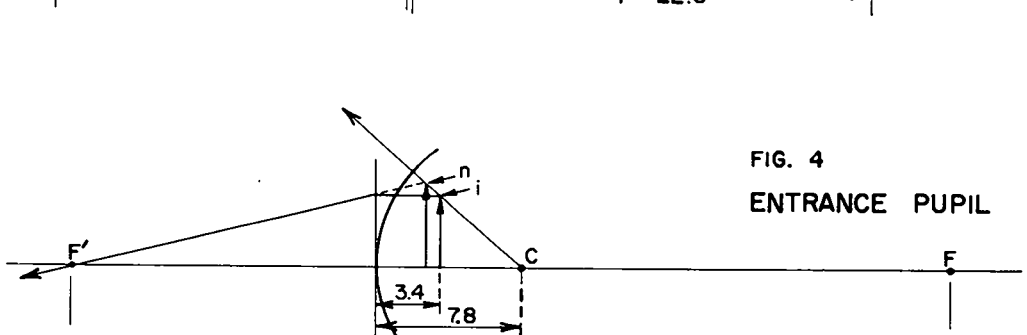

FIG. 4

ENTRANCE PUPIL

FIG. 5

EXIT PUPIL

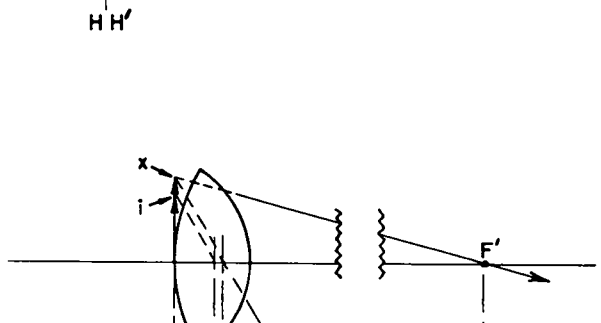

For calculational purposes it is convenient to introduce a simpler model of the eye known as a reduced eye. This consists of a single refracting surface separating air from a homogeneous medium of index n′. For such a system, the principal planes are both at the vertex of the interface, and the nodal points are both at the center of curvature of the interface (Fig. 7). In order that this reduced eye correspond to the schematic eye as nearly as possible, the parameters of the former are determined as follows:

(a) In order that the image size be the same in both eyes we must have $\overline{N'F'} = 17.1$ (and hence also f = 17.1).

(b) The wavelength of light in the medium n′ should be the same as in the vitreous humor in order that diffraction effects should be the same; hence $n' = 4/3$, and $\overline{H'F'} \equiv f' = n'f = 22.8$. The radius of curvature of the interface is thus 5.7mm.

(c) In order that diffraction and chromatic-aberration effects be the same, the exit pupil (in this case, also the physical iris) should be still 21.2mm from the retina, and the same size as before. This places the entrance pupil

$$\frac{22.8 \cdot 17.1}{21.2} = 18.4\text{mm}$$

to the right of F, or 0.3mm in front of the exit pupil, with

$$\frac{r_n}{r_x} = \frac{4.4}{4.1} = 1.07 \ .$$

FIG. 6

SCHEMATIC EYE

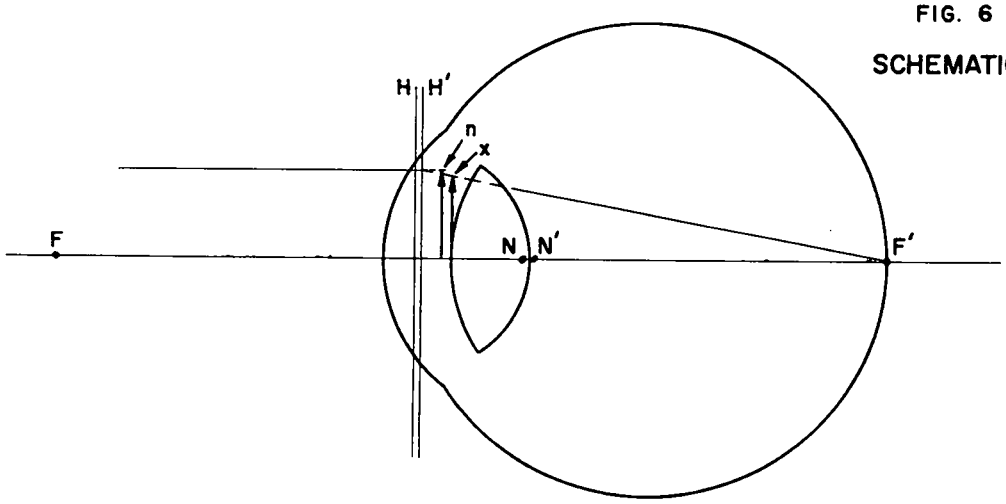

FIG. 7

REDUCED EYE

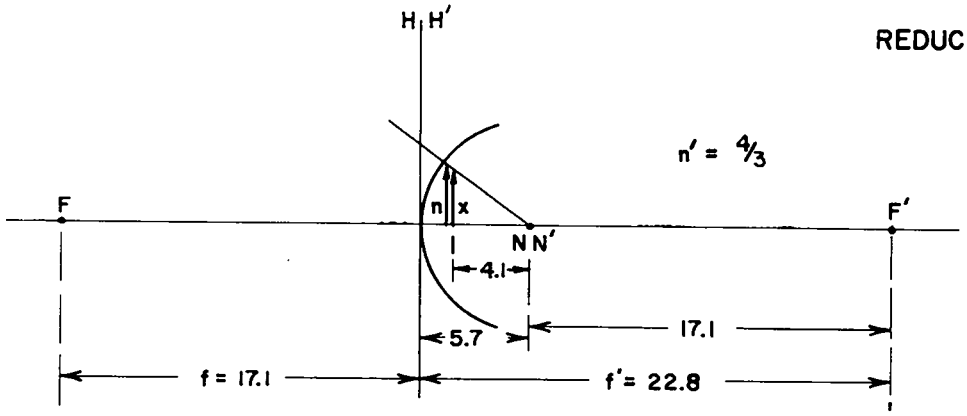

FIG. 8

SIMPLIFIED REDUCED EYE

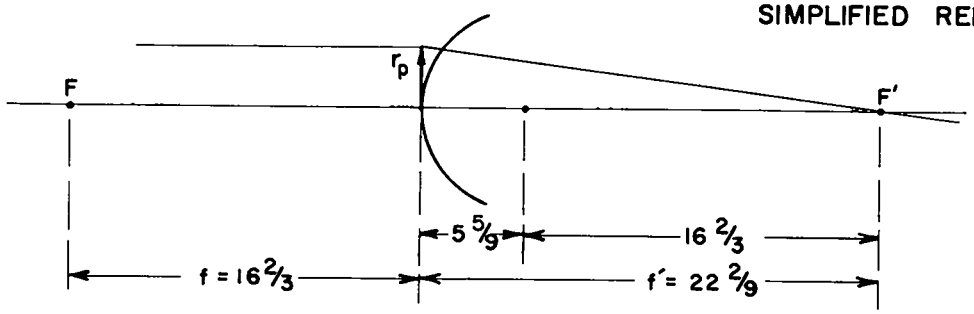

Thus the entrance pupil is almost exactly the proper diameter, and the proper amount of light is allowed to enter the eye.

We now simplify our eye model still further by noting that the interface is just seven percent farther from the retina than is the exit pupil in Fig. 7. Thus if we move the physical iris to the interface and increase its radius seven percent, the entrance pupil (now coincident with iris and exit pupil) has the proper size, and the diffraction effects have not been changed (since they depend only on the angle subtended by r_x at F'). This modification does change the effects of chromatic aberration (blurring of the retinal image for wavelengths other than that at which the eye is focussed), but the magnitude of the error for a given wavelength is less than a percent and the direction is opposite for longer and shorter wavelengths, so that the net error for white light is very small.

To be slightly more conservative, we shall actually use for most calculations the model shown in Fig. 8, with $f = 16\frac{2}{3}$mm. This change reduces the radii of the geometrical and diffraction images by about three percent, leaving the chromatic aberration unaffected (for a given value of the parameter S to be defined later), and making the power of the eye a round

$$P = \frac{1000}{16\frac{2}{3}} = 60 \text{ diopters} .$$

We shall for the present assume that the interface has a nonspherical

form such as to essentially eliminate spherical aberration.

B. I(r) and a_o for Diffraction Only

We consider first the case of a geometrically perfect eye, in which the form of the point-source image-spread function I(r) is determined solely by diffraction effects. For a circular pupil and monochromatic light of wavelength λ in air, I(r) is the well-known Airy diffraction pattern[14]

$$I(r) = [2J_1(v)/v]^2 , \tag{37}$$

where $J_1(v)$ is the Bessel function of order 1 and

$$v = \frac{2\pi\, r_p r}{\lambda' f'} = \frac{2\pi\, r_p r}{\lambda f} , \tag{38}$$

r_p being the pupil radius and $\lambda' = \lambda/n'$ the wavelength in the medium of index n'. (Note that the size of the diffraction pattern depends on $\lambda' f' = \lambda f$, and thus is the same as though it were produced in air by a thin lens of focal length f.) The total power in the pattern I(r) is proportional to[14]

$$\int_0^\infty I(r) v\, dv = \int_0^\infty \left[\frac{2J_1(v)}{v}\right]^2 v\, dv = 2 . \tag{39}$$

The effective radius is thus given by

$$\int_0^{v_o} v\, dv = \frac{v_o^2}{2} = 2 , \qquad \text{or} \quad v_o = 2 . \tag{40}$$

For a 4mm-radius pupil and $\lambda = 5500\text{Å}$,

$$a_o = \frac{\lambda f\, v_o}{2\pi\, r_p} = \frac{0.55\mu \cdot 16.7\text{mm} \cdot 2}{2\pi \cdot 4\text{mm}} = 0.73\mu . \tag{41}$$

The function g is[14]

$$g(a/a_o) = g(v/2) = 1 - J_o^2(v) - J_1^2(v) . \tag{42}$$

Neglecting chromatic aberration, the image-spread function for the entire visible spectrum is given simply by averaging (37) appropriately. Since λ changes by only about ±30 percent from the mean value 0.55μ, it is clear there will be no large change from the monochromatic case. However, results calculated for a $v\, dv$ spectrum with the aid of a code to be described below are shown in Figs. 9 and 10, along with the monochromatic results (37)-(42); the smaller value $a_o = 0.62\mu$ is due to the heavy weighting of shorter wavelengths. It may be noted that the g functions lie fairly close to the rough function (27) of Fig. 2, and that the values

$$a_o/r_h \cong 1.24\text{-}1.28$$

are close to the value 1.3 assumed at the end of Sec. 3. However, the

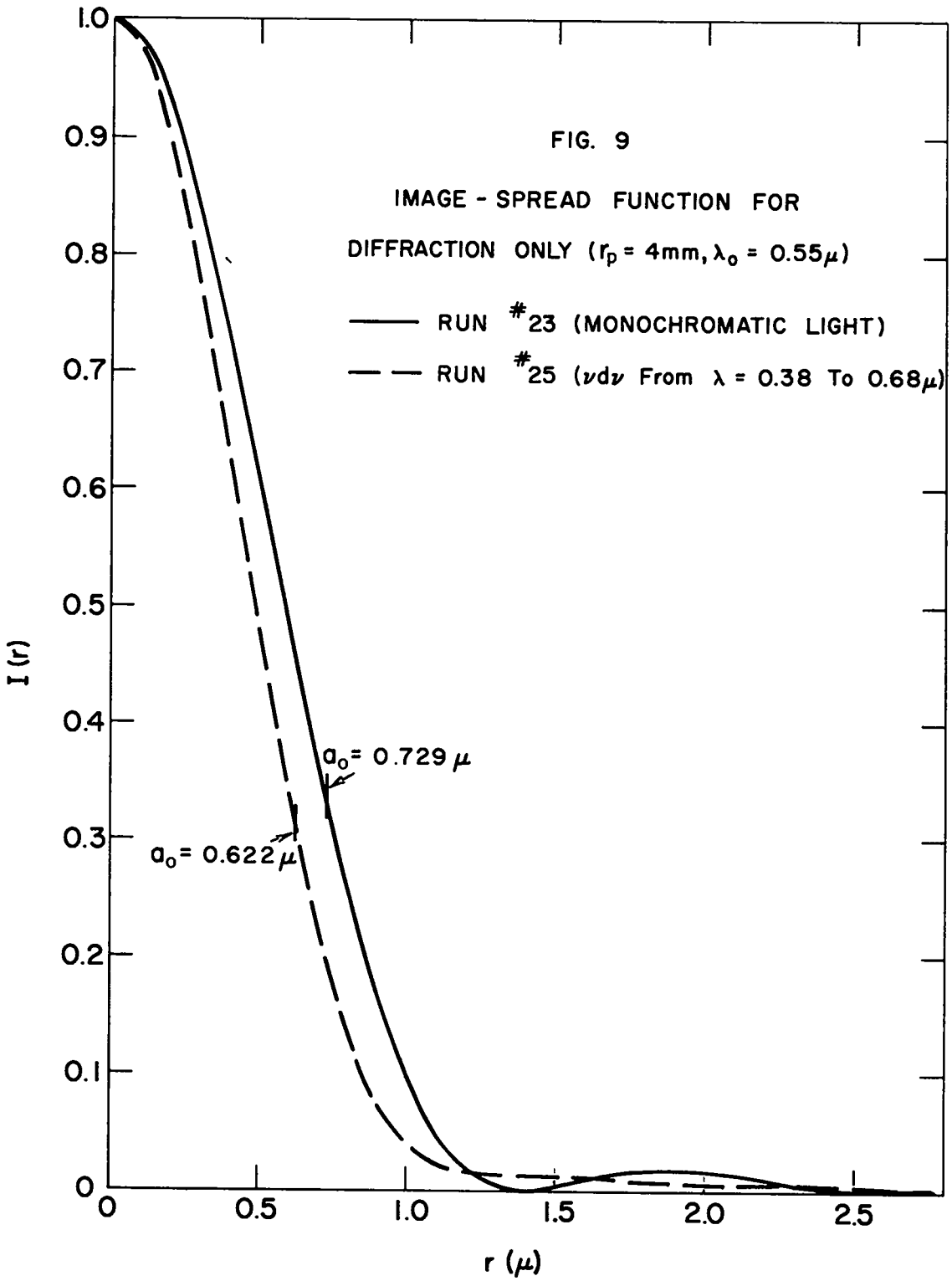
FIG. 9
IMAGE - SPREAD FUNCTION FOR
DIFFRACTION ONLY (r_p = 4mm, λ_0 = 0.55μ)
RUN #23 (MONOCHROMATIC LIGHT)
RUN #25 ($\nu d\nu$ From λ = 0.38 To 0.68μ)
a_0 = 0.729 μ
a_0 = 0.622 μ
I (r)
r (μ)
1.0
0.9
0.8
0.7
0.6
0.5
0.4
0.3
0.2
0.1
0
0.5
1.0
1.5
2.0
2.5

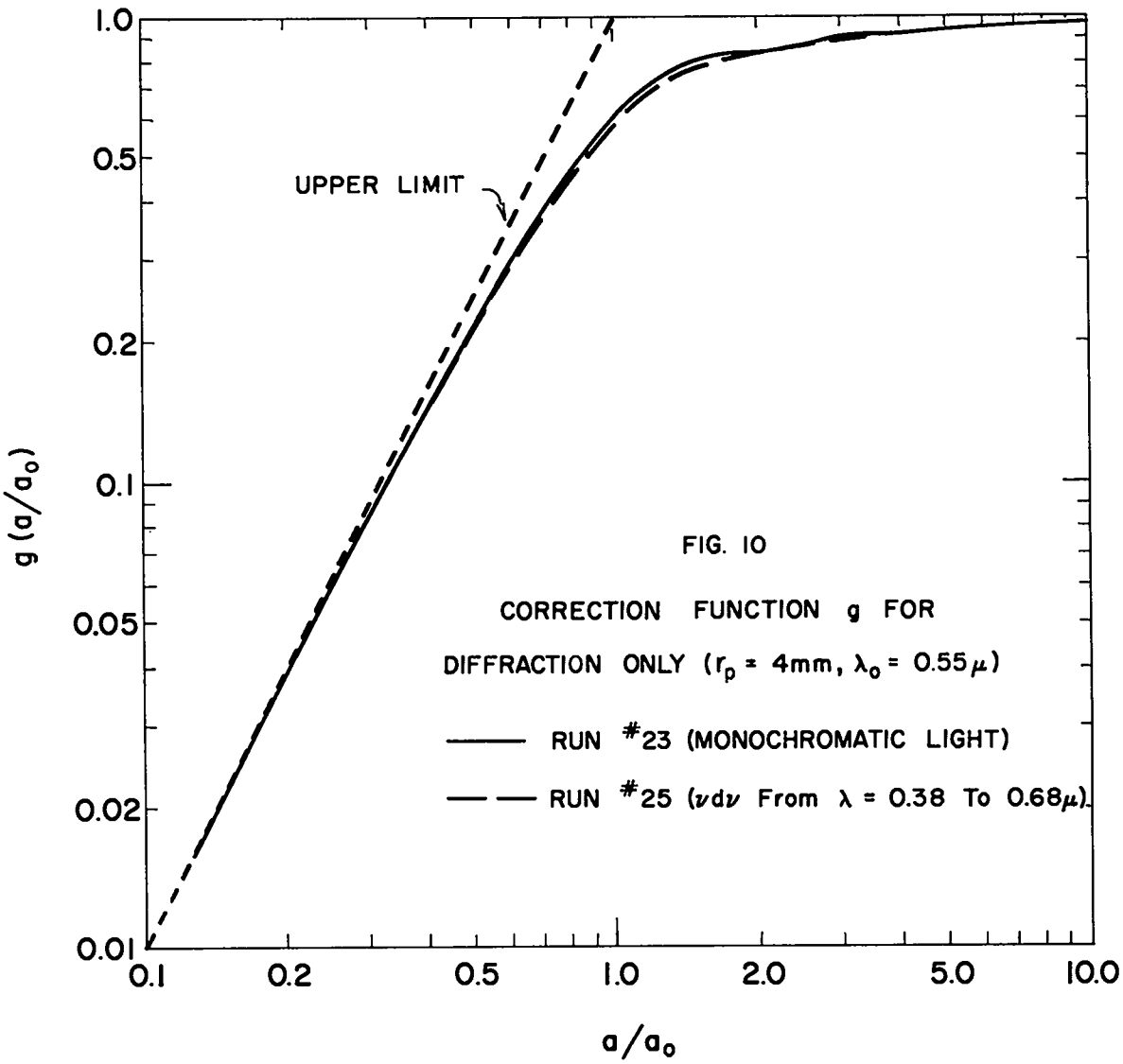
1.0
0.5
0.2
0.1
0.05
0.02
0.01
g (a/a₀)
UPPER LIMIT
0.1
0.2
0.5
1.0
2.0
5.0
10.0
a/a₀
FIG. 10
CORRECTION FUNCTION g FOR
DIFFRACTION ONLY (r_p = 4mm, λ₀ = 0.55μ)
RUN #23 (MONOCHROMATIC LIGHT)
RUN #25 (νdν From λ = 0.38 To 0.68μ)

absolute result $a_o \cong 0.6\text{-}0.7\mu$ is an order of magnitude below the value $a_o = 6\mu$ derived there from experiment; it is indeed so small that one would be in very serious trouble with eyeburn if the eye were really geometrically perfect. Fortunately, there is every indication that the eye is replete with optical imperfections.

C. Chromatic Aberration of the Eye

It has long been known that the eye shows considerable chromatic aberration. Helmholtz,[15] for example, quotes experiments by himself, by Fraunhofer, and by Matthiessen indicating that the mean dispersion of the ocular media is somewhat greater than that of water, and points out that this is reasonable since the index of refraction of the lens is appreciably greater than that of water (high dispersion tending to go with high n). This argument is supported by the fact that the transmission of the eye in the ultraviolet cuts off much more sharply and at longer wavelengths than does a 25mm thickness of water (UV absorption bands being the usual cause of dispersion in the visible); details are given in Fig. 11[16] and Table II.

Also given in Table II are powers calculated from

$$f = R/(n' - 1) \tag{43}$$

for the reduced eye of Fig. 8 when the refracting medium n' is water; it is seen that the power of the eye may be expected to vary by more than two diopters over the visible region.

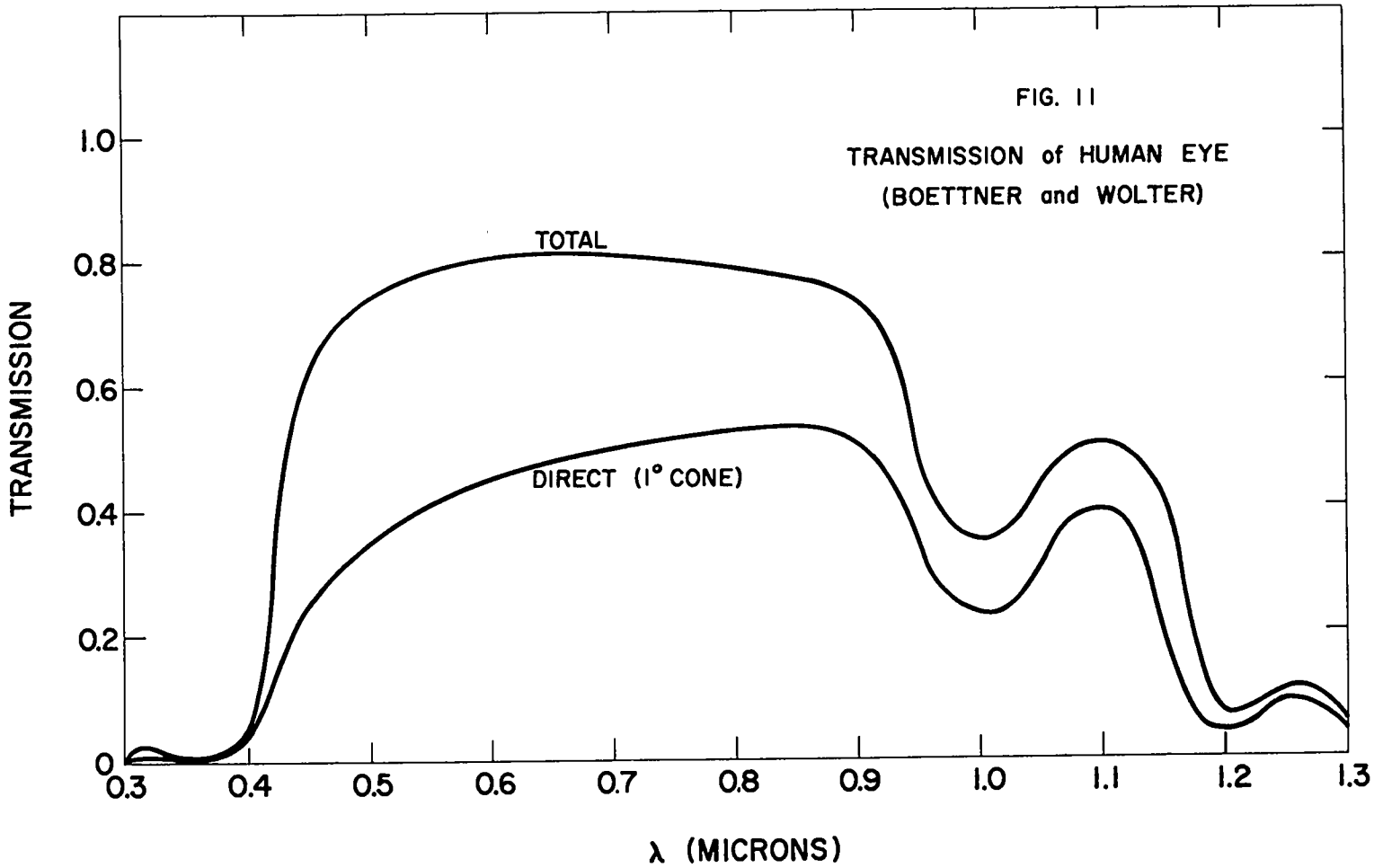
FIG. 11
TRANSMISSION of HUMAN EYE
(BOETTNER and WOLTER)
TOTAL
DIRECT (1° CONE)
TRANSMISSION
λ (MICRONS)
0
0.2
0.4
0.6
0.8
1.0
0.3
0.4
0.5
0.6
0.7
0.8
0.9
1.0
1.1
1.2
1.3

TABLE II

TRANSMISSION OF WATER AND THE HUMAN EYE, AND DISPERSION OF WATER

λ	ϵ_{H_2O} [a]	$T_{H_2O} = e^{-2.5\epsilon}$	T_{eye} [b]	n_{H_2O} [c]	$P_{H_2O} = \frac{n-1}{R}$
0.2μ	0.08 cm^{-1}	0.82	0		
0.3	0.0064	0.98	0		
0.397	0.0008	0.998	0.06	1.3411	61.40 diop
0.434	0.0005	0.999	0.50	1.3380	60.84
0.486	0.0004	0.999	0.72	1.3349	60.28
0.589	0.0018	0.995	0.80	1.3307	59.53
0.656				1.3290	59.22
0.7	0.0058	0.985	0.80		
0.8	0.024	0.942	0.79		
0.9	0.06	0.86	0.74		
0.95	0.3	0.47	0.48		

[a] Smithsonian Physical Tables, p. 536 (T = 20°C).

[b] Reference 16.

[c] Amer. Inst. of Phys. Handbook, p. 6-90 (T = 40°C).

A number of fairly extensive sets of subjective measurements of the chromatic aberration of the human eye have been made,[17-21] and the results are commonly presented in the form of the dioptric power ΔP_s of a supplementary lens at the cornea required to correct the eye at each of a number of wavelengths. In Fig. 12, we show the negative of these corrective powers (relative to $\lambda_o = 0.55\mu$) plotted against ν^2, where

$$\nu = 1/\lambda \ . \tag{44}$$

The plotted points are values averaged over all eyes of a given investigation, and the dashed lines give the approximate range of the results measured for the individual observers of Wald and Griffin and of Bedford and Wyszecki.

It must be noted that $-\Delta P_s$ is <u>not</u> the same as the change $\Delta P_e = \Delta(1/f_e)$ in the power of the eye referred to air nor the change $\Delta P'_e = \Delta(1/f'_e)$ in the power of the eye referred to the medium n', but is more nearly the geometrical mean of the two. This may be seen as follows for the reduced eye: The imaginary supplementary lens produces an image at a distance $f_s = 1/P_s$ to the right of the cornea. The object distance p_e for the eye is then $-f_s$ (neglecting the distance between cornea and first principal plane), so that from (36) the image distance q_e is given by

$$\frac{f_e}{p_e} + \frac{f'_e}{q_e} = 1 \ ,$$

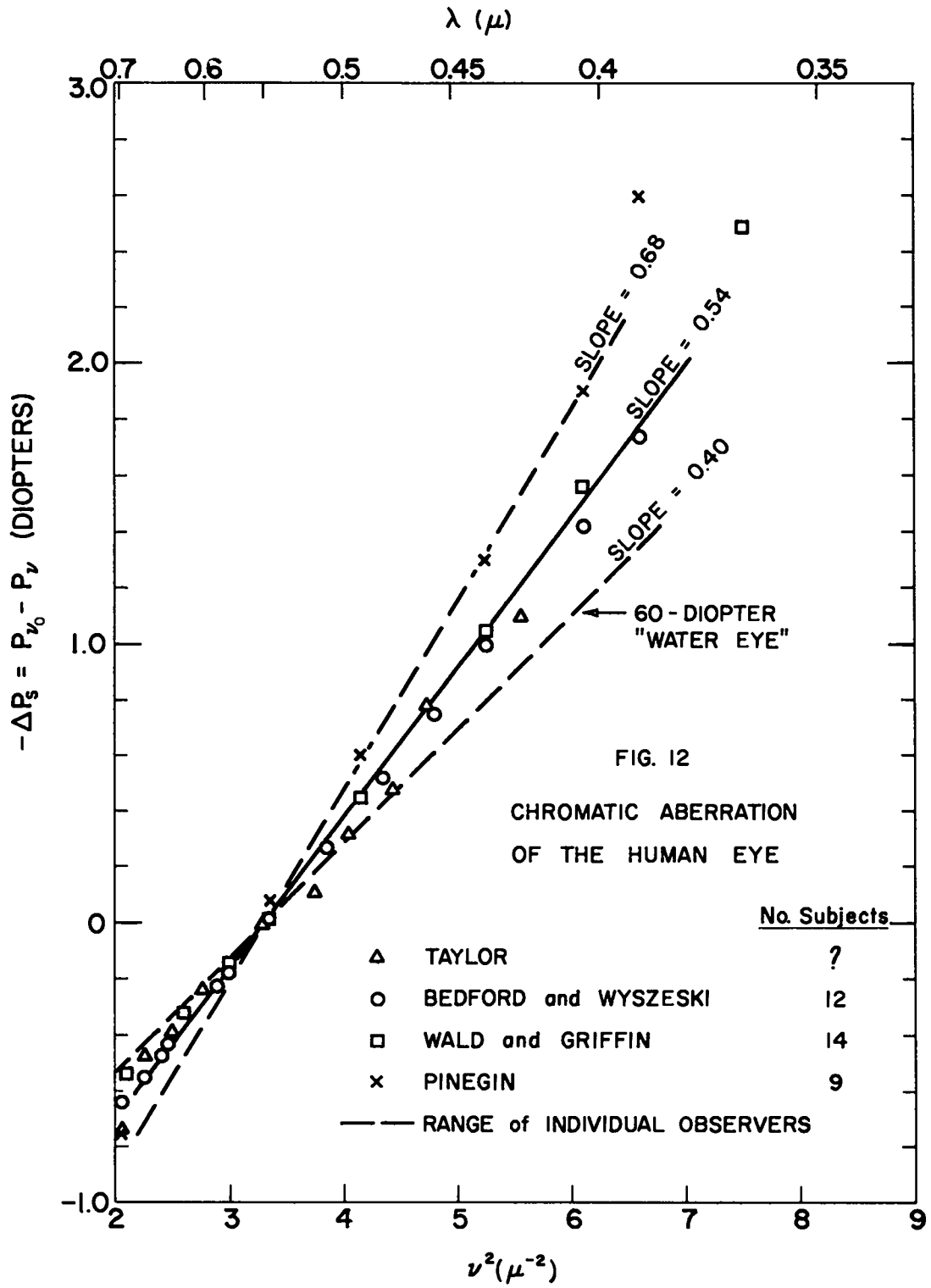
λ (μ)
0.7
0.6
0.5
0.45
0.4
0.35
3.0
2.0
1.0
0
-1.0
$-\Delta P_s = P_{\nu_0} - P_\nu$ (DIOPTERS)
SLOPE = 0.68
SLOPE = 0.54
SLOPE = 0.40
60 - DIOPTER "WATER EYE"
FIG. 12
CHROMATIC ABERRATION OF THE HUMAN EYE
No. Subjects
TAYLOR ?
BEDFORD and WYSZESKI 12
WALD and GRIFFIN 14
PINEGIN 9
RANGE of INDIVIDUAL OBSERVERS
2
3
4
5
6
7
8
9
$\nu^2(\mu^{-2})$

$$-P_s = \frac{1}{f_e} - \frac{f'_e}{q_e f_e} = P_e - \frac{n'}{q_e} .$$

For the reduced eye, q_e is constant in these experiments, so that

$$-\Delta P_s = \Delta P_e - (\Delta n')/q_e ,$$

which shows that ΔP_e is <u>not</u> the negative of ΔP_s.

From (43),

$$P_e = (n' - 1)/R \tag{45}$$

so that

$$\Delta n' = R\ \Delta P_e ,$$

and

$$-\Delta P_s = \left(1 - \frac{R}{q_e}\right)\Delta P_e = \frac{f_o}{f'_o}\ \Delta P_e = \frac{1}{n'_o}\ \Delta P_e , \tag{46}$$

where the zero subscripts refer to the wavelength λ_o of normal focus of the eye. It is easily seen from (45) and the relation $P_e = n'P'_e$ that

$$\frac{1}{n'}\ \Delta P_e = n'\Delta P'_e , \tag{47}$$

whence the relation

$$-\Delta P_s \cong [(\Delta P_e)(\Delta P'_e)]^{1/2} \qquad (48)$$

follows. This analysis for the reduced eye of Fig. 8 is only an approximation to the more realistic eye of Fig. 6, but a detailed calculation for the latter (given in the appendix) shows that no error is introduced into what follows [specifically, Eq. (62)].

The quantity $(\Delta P_{H_2O})/n'_o$, calculated from Table II and representing the chromatic correction $-\Delta P_s$ which would be measured for a 60-diopter "water eye," is essentially coincident with the dashed curve of Fig. 12 having a slope of 0.40. As anticipated above, the experimentally measured slopes are indeed mostly greater than this. The spread in the experimental data is, however, rather mysterious until it is noted that these slopes are a measure of chromatic aberration and not inherent dispersion: (45) shows that $S \equiv -dP_s/d(\nu^2)$ is proportional not only to $dn'/d(\nu^2)$ but also to R^{-1} and hence (for given n'_o) to the mean power of the eye at ν_o. As will be discussed later in greater detail, normal emmetropic eyes vary in (unaccommodated) power by about ±10 percent from the average value of 58^+ diopters.[22,23] Taking into account ametropic eyes which have been focussed by accommodation and/or correction with spectacle lenses, the powers of the eyes used in the experimental investigations could have covered a range of up to ±15 percent.[22,23] This would represent a good portion of the observed spread of ±25 percent; the remainder could well represent scatter in the experimental measurements, or systematic error due to unconscious partial compensation

by some subjects in not accommodating simultaneously to both monochromatic and white-light objects.

Since 60 diopters is somewhat higher than the average refractive power of the human eye, it follows from (46) and Fig. 12 that the value

$$S = (1/n_o')dP_e/d(\nu^2) = 0.40 \text{ diopter} - \mu^2 \qquad (49)$$

should almost certainly represent a conservative value for the chromatic aberration of a 60-diopter human eye, and that a value 0.54 is probably realistic.

For a slope of 0.40 and an eye focussed at $\lambda = 0.5\mu$, it may be noted from Fig. 12 that ΔP_s covers about the range ± 0.8 diopters over the visible spectrum. From (46) and (47), this means

$$P_e' \cong 45 \pm 0.6 \text{ diopters}$$

or

$$f_e' \cong 22.2 \pm 0.3\text{mm} ,$$

so that the axial chromatic aberration of the human eye amounts to something like

$$\Delta f_e = \Delta f_e' = \pm 300\mu \qquad (50)$$

(or more, for larger S).

D. I(r) and a_o for Diffraction plus Chromatic Aberration

We now calculate the point-source image-spread function for non-monochromatic light, including the effects of chromatic aberration. We suppose that at some given layer within the retina, the eye (again assumed geometrically perfect) is in focus for some wavelength λ_o, or wavenumber $\nu_o = 1/\lambda_o$. (For the layer most pertinent to distinct vision, this wavelength is about 0.56μ under conditions of bright illumination and about 0.50μ for dim light.[18]) For a point source, light of this wavelength will fall on this layer of the retina in the intensity pattern given by (37). Because of chromatic aberration, light of some other wavelength $\lambda = 1/\nu$ will be out of focus at this layer of the retina. Its intensity pattern will not be the usual Airy (Fraunhofer-diffraction) pattern, but will be a more complicated out-of-focus (Fresnel-diffraction) pattern of the type shown in Cagnet, et al.[24] The intensity function has been calculated theoretically by Lommel;[25] details can be found conveniently in Born and Wolf:[26]

One introduces dimensionless variables

$$u = \frac{2\pi\, r_p^2(f_o' - f')}{\lambda' f'^2} = \frac{2\pi\, r_p^2(f_o' - f')}{\lambda f\, f'}\,, \tag{51}$$

$$v = \frac{2\pi\, r_p r}{\lambda' f'} = \frac{2\pi\, r_p r}{\lambda f}\,, \tag{52}$$

measuring respectively the distance from the geometrical focal plane, and

radial distance from the center of the diffraction pattern; the boundary of the geometrical shadow is given by $v = |u|$. Defining the Lommel functions

$$U_n(u,v) = \sum_{s=0}^{\infty} (-1)^s (u/v)^{n+2s} J_{n+2s}(v) , \tag{53}$$

$$V_n(u,v) = \sum_{s=0}^{\infty} (-1)^s (v/u)^{n+2s} J_{n+2s}(v) , \tag{54}$$

then the intensity pattern $I(u,v)$ normalized to unity at the geometrical focus $[I(o,o) = 1]$ is given by either of the expressions

$$I(u,v) = (2/u)^2 \{U_1^2(u,v) + U_2^2(u,v)\} , \tag{55}$$

$$I(u,v) = (2/u)^2 \Big\{ 1 + V_o^2(u,v) + V_1^2(u,v) - 2V_o(u,v) \cos\left(\frac{u}{2} + \frac{v^2}{2u}\right) - 2V_1(u,v) \sin\left(\frac{u}{2} + \frac{v^2}{2u}\right) \Big\} , \tag{56}$$

the former being more rapidly convergent for $u < v$, and the latter for $u > v$. It is easily seen from (53) that in the focal plane $u = 0$, (55) reduces to the correct Airy result (37). Since (55)-(56) represent the same total power at any plane $u =$ constant, it then follows from (39) that

$$\int_0^{\infty} I(u,v) v \, dv = 2 \tag{57}$$

for all values of u.

A contour plot of the function (55)-(56) may be seen in Born and Wolf.[26] The form of I(u,v) for various u (adapted from Hopkins[27]) is shown in Fig. 13; also plotted are rectangles showing the geometrical intensity, which from (57) is

$$I_{geom} = \begin{cases} \frac{4}{u^2}, & v \leq v_{geom} = u, \\ \\ 0, & v > u. \end{cases} \tag{58}$$

There are three points here worthy of special notice: (1) The strong central diffraction peak persists with only moderately reduced intensity to planes as far out of focus as $|u| = 2\pi$. (For $f'/r_p \cong 5.5$, this means $|f'_o - f'| \cong 30\lambda' \cong 12\mu$.) (2) I(u,v) does not begin to approximate I_{geom} until at least $u = 8\pi$; i.e., until the eye is out of focus by at least 120 wavelengths $\cong 50\mu$. [This is more than ten percent of the total variation (50) in the focal length of the eye.] (3) Along the symmetry axis v = 0, I(u,o) <u>never</u> approximates the geometrical value: From (54) and (56)

$$I(u,o) = (2/u)^2\{2 - 2\cos(u/2)\}$$

$$= \frac{\sin^2(u/4)}{(u/4)^2}, \tag{59}$$

so that the intensity varies along the axis between 0 and $4I_{geom}$, with an average value of $2I_{geom}$; this is related to the fact that we are dealing with coherent light, where <u>amplitudes</u> add (giving resultant amplitudes, as the phases vary, between 0 and 2 times the geometrical value).

For a polychromatic point source of the sort of interest to us here, light of different wavelengths is noncoherent and the total intensity at the retinal layer in question is given by an appropriately weighted integral of $I(u,v)$ over the pertinent frequency range. The required expression is found as follows.

Let the intensity of the light falling on the entrance pupil and having frequencies between ν and $\nu + d\nu$ be $W(\nu)\, d\nu$. Then the total power passing through the pupil is $\pi\, r_p^2 W\, d\nu$. If the intensity in the plane u is $I_\nu(r)\, d\nu = C\, I(u,v)\, d\nu$ then conservation of energy requires that

$$\pi\, r_p^2 W(\nu) = \int_0^\infty I_\nu(r) 2\pi\, r\, dr$$

$$= 2\pi\, C(\lambda f/2\pi\, r_p)^2 \int_0^\infty I(u,v) v\, dv\ ,$$

so that from (57)

$$I_\nu(r) = (\pi\, r_p^2/\lambda f)^2 I(u,v) W(\nu)\ . \qquad (60)$$

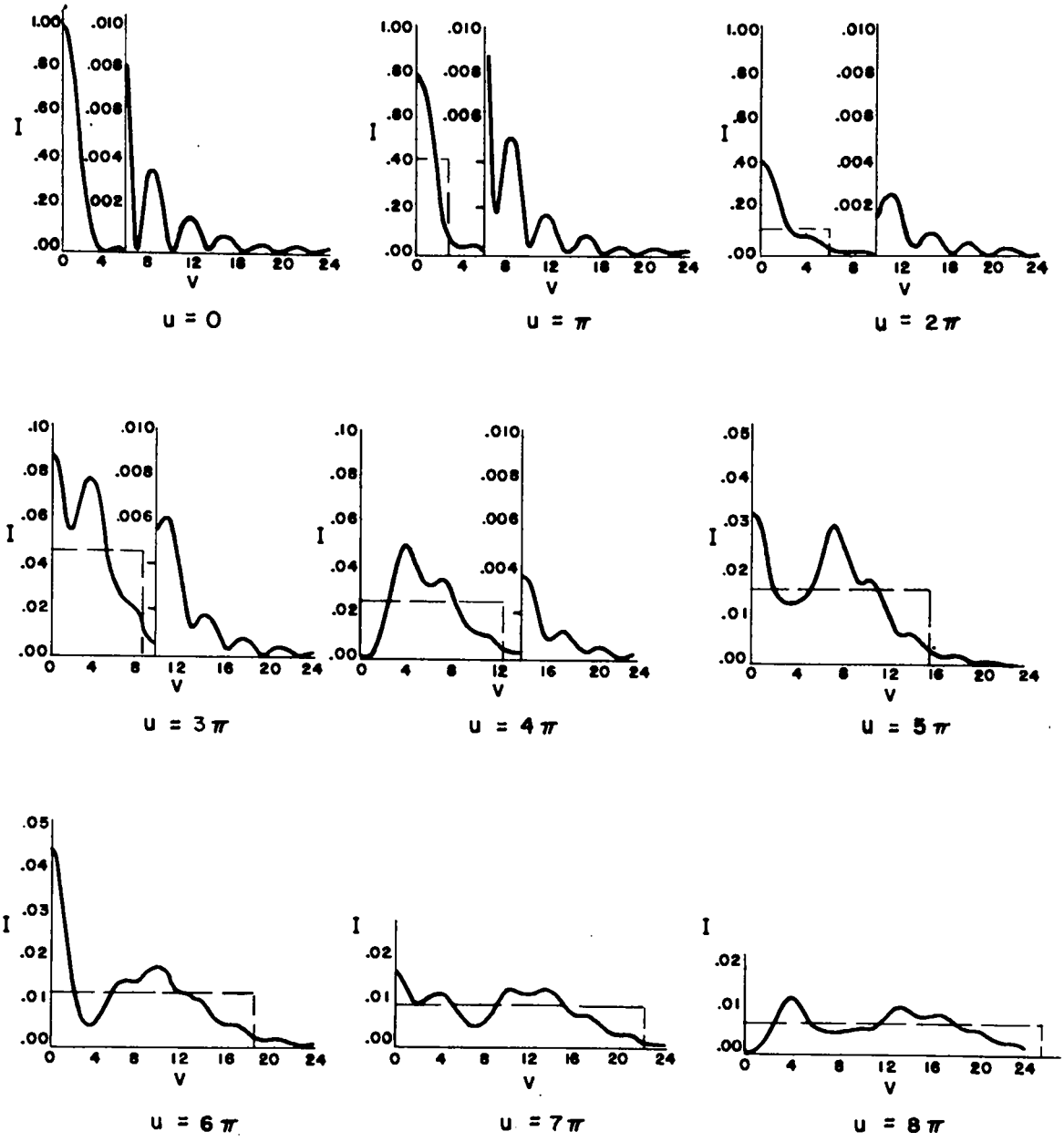

FIG. 13

OUT-OF-FOCUS DIFFRACTION PATTERNS

The total intensity I(r) for the polychromatic source is the frequency integral of (60) for fixed r and observational plane. The manner in which u and v vary with frequency may be expressed in terms of the power of the eye P_o at the frequency of focus ν_o and the power P at frequency ν: From (46) and the approximate straight-line nature of Fig. 12,

$$P \equiv P_o + P_1 \cong P_o + n_o' S(\nu^2 - \nu_o^2) \ , \tag{61}$$

where a typical value of the slope S is given by (49). From (47), (51), and (52)

$$u = \frac{2\pi\ r_p^2 f_o'}{\lambda f}\left(\frac{1}{f'} - \frac{1}{f_o'}\right) \cong \frac{2\pi\ r_p^2 f_o}{\lambda f\ n_o'}\ (P - P_o)$$

$$= \frac{2\pi\ r_p^2 \nu\ P\ P_1}{P_o n_o'} = \frac{2\pi\ r_p^2 \nu\ P\ S}{P_o}\ (\nu^2 - \nu_o^2\ ) \ , \tag{62}$$

$$v = 2\pi\ r_p \nu\ P\ r \ . \tag{63}$$

With u and v given by these expressions, the image-spread function is

$$I(r) = \pi^2 r_p^4 \int_{\nu_1}^{\nu_2} \nu^2 P^2 I(u,v) W(\nu)\ d\nu \ . \tag{64}$$

From the behavior of I(u,v) discussed in connection with Fig. 13, we may anticipate that I(r) will tend to show a narrow peak at r = 0

(with half-width of about $v = 2$, or $r \cong 0.7\mu$) which projects considerably above the surrounding (semi-geometrical-average) background. Possibly it is this very fine central diffraction peak which is associated with the high visual acuity (about one micron) of good eyes; the much broader "background" illumination in I(r) for larger r, however, results in values of a_o of several times this, as we shall now show.

For $r_p = 4\text{mm}$, $v \cong 2\mu^{-1}$, $P \cong P_o = 60$ diopters, and radii to perhaps $r = 20\mu$, it follows from (62)-(63) that values of

$$u \cong 150P_1 (\cong -200P_s) \tag{65}$$

as large as ±200, and values of

$$v \cong 3r \tag{66}$$

out to 60 are involved in the evaluation of (64). These are quite large ranges, over which the function I(u,v) varies in a very complicated manner, and it is difficult to do much in the way of calculating I(r) analytically. However, it <u>is</u> easy to estimate I(o) and the value of a_o. From (64) and (59),

$$I(o) = \pi^2 r_p^4 \int_{v_1}^{v_2} v^2 P^2 \frac{\sin^2 (u/4)}{(u/4)^2} W(v)\, dv \ .$$

Now $W(v)$ is generally a relatively flat function and it may then be easily shown that more than 90 percent of the contribution to this

integral comes from the region $|u| < 20$, or from (65), $|P_s| < 0.1$. From Fig. 12 it may be seen that v varies only about ±6 percent over this range, so that to a very good approximation

$$I(o) \cong \frac{\pi\, r_p^2 p_o^2 W(v_o)}{S} \int_{u_1/4}^{u_2/4} \frac{\sin^2 (u/4)}{(u/4)^2}\, d(u/4)$$

$$\cong \pi^2 r_p^2 p_o^2 W(v_o)/S \ , \tag{67}$$

since $u_2 \cong -u_1 \cong \infty$ so far as this integral is concerned. From (64), (63), and (57), the total power is

$$\int_0^\infty I(r) 2\pi\, r\, dr = \frac{\pi\, r_p^2}{2} \int_{v_1}^{v_2} W(v) \int_0^\infty I(u,v) v\, du\, dv$$

$$= \pi\, r_p^2 \int_{v_1}^{v_2} W(v)\, dv \ , \tag{68}$$

as follows also from the definition of $W(v)$. Then from the definition of a_o, Eq. (8), we find

$$a_o = \frac{f_o}{\pi} \left\{ \frac{S}{W(v_o)} \int_{v_1}^{v_2} W(v)\, dv \right\}^{1/2} , \tag{69}$$

or

$$a_o = \frac{f_o}{\pi}\left\{\frac{\bar{W}}{W(\nu_o)}\, S(\nu_2 - \nu_1)\right\}^{1/2}$$

$$\cong \frac{f_o}{\pi}\{S(\nu_2 - \nu_1)\}^{1/2} , \qquad (70)$$

since the mean value $\bar{W}$ is not greatly different from the value of W at the in-focus frequency ν_o. For $f_o = 16.7\text{mm} = 1.67 \cdot 10^4\mu$, S = 0.40 diopter - $\mu^2 = 0.40 \cdot 10^{-8}\mu$, $\nu_2 = 1/0.4 = 2.5\mu^{-1}$, and $\nu_1 = 1/0.7 = 1.43\mu^{-1}$,

$$a_o \cong \frac{1.67 \cdot 10^4}{\pi}\{0.40 \cdot 10^{-8} \cdot 1.07\}^{1/2} = 3.4_8\mu . \qquad (71)$$

This is appreciably smaller than the value 6.4μ deduced from experiment in Sec. 3, but is much larger than the theoretical value 0.6μ obtained in Sec. 4B for diffraction only, and shows the importance of chromatic aberration. There are a number of interesting features of the above analytic results:

(a) I(o) depends on the entrance-pupil radius r_p only insofar as the total energy passing through is thereby changed; thus with an increase in r_p, the increase in I(o) to be expected because of lower diffraction spreading is exactly cancelled (in this approximation) by the increasing effect of chromatic aberration.

(b) I(o) is approximately independent of the width of spectrum assumed; this is because once the frequency differs from ν_o by more than

about ten percent ($|P_s| \cong 0.3, |u| \cong 60$), the geometrical intensity (58) has been so reduced by chromatic aberration that there is essentially no further contribution to I(o).

(c) $I(o) \propto P_o^2 = 1/f_o^2$, simply because of the proportionality of image size to f_o.

(d) $I(o) \propto 1/S$, because the greater the chromatic dispersion, the shorter the frequency range $|\Delta\nu| = |\Delta P_s/2S\ \nu_o|$ which contributes appreciably to I(o).

(e) $a_o \propto f_o S^{1/2}$ because of the greater spreading of the image, as in (c) and (d).

(f) $a_o \propto (\nu_2 - \nu_1)^{1/2}$ because, as pointed out above, increasing the spectral range adds almost nothing to I(o), but it does contribute linearly (for W = const) to the total energy in the image for which a_o^2 must account. <u>This point is very important</u>; it means that for eyeburn purposes it does not matter much what spectral range of the source one considers (as long as it covers at least $\nu_o \pm 0.1\nu_o$) provided one uses the value of a_o appropriate to that spectral range. For example, we may calculate the eyedose using a source-brightness history determined from photographic records provided only that we use the value of a_o appropriate to the film's sensitivity range ($\sim$0.38 - 0.68μ), and regardless of the fact that the eye transmits appreciably out to about 1.4μ. (It is assumed, of course, that there is no partial correction of chromatic aberration which brings the light back into focus again at some wavelength other than λ_o.) Actually, these last remarks are just a first

approximation, valid only for unresolved sources (geometrical radii $a \ll a_o$). For sources large enough to be partially resolved, the detailed form of I(r) -- through its integral $g(a/a_o)$ -- is also of importance, and this function will be different when calculated for different spectral ranges.

As mentioned earlier, I(r) is not easily found analytically. Therefore a Fortran code RCØ for the IBM 7094 has been developed to calculate I(r) numerically:

The integral (64) for I(r) is evaluated using Simpson's rule over an equal-frequency-interval mesh (250 intervals being usually used when the wavelength range is 0.1μ or more). This is done for each of 48 values of the radius, r = 0(0.1)1.0(0.25)3.0(0.5)14(1)21μ. For each (v,r), values of (u,v) are found from (61)-(63), and I(u,v) then evaluated from (53)-(56) [using a very convenient subroutine which evaluates $J_n(v)$ for all required n from simple recursion and normalization relations]. The total-power integral (68) is evaluated similarly to I(r), and a_o then found from (8). With I(r) found for all r, the code calculates

$$\int_0^a I(r) r \, dr \ ,$$

using the trapezoidal rule for values of a on the same mesh as r, whence $g(a/a_o)$ follows from (6).

Input parameters to the code are f_o, r_p, S, λ_o, λ_1, λ_2, the number of frequency intervals to be used in the integration mesh, and parameters needed to calculate the spectral distribution function, which is taken to be

$$W(\nu) = \frac{\nu^n}{1 + b \cdot |\nu - \nu_c|^m} \cdot \tag{72}$$

Nonzero values of b and m may be used to approximate filtered spectra peaked at λ_c, such as those used in some of the experimental image-spread measurements. Normally, however, b is set to zero, whence

$$W(\nu) = \nu^n ;$$

n = 2 corresponds to the high-temperature (Rayleigh-Jeans) limit of the black-body spectrum, n = -1 or -2 to a solar-like spectrum, and n = 1 or 1.5 is a good average for temperatures of 1 to 5 volts, typical of high-altitude explosions at times pertinent to the eyeburn problem.

Calculating times on the 7094 average about 2.2 minutes per case for a 250-interval frequency mesh. Sample results for a_o are given in Table III, where they are compared with the analytical expression (69). It may be seen that the latter is quite accurate, and can therefore be used for all reasonable cases [$W(\nu)$ comparable to $W(\nu_o)$ over a range at least $\nu_o \pm 0.1\nu_o$, at which points $u \geq 16$; i.e., $r_p \geq 2$mm for $S \geq 0.4$ diopter - μ^2, or $r_p \geq 3$ for $S \geq 0.2$].

TABLE III

VALUES OF a_o FROM MACHINE CALCULATION, DIFFRACTION PLUS CHROMATIC ABERRATION

Run no.	f_o(mm)	r_p(mm)	S	$\lambda_1(\mu)$	$\lambda_2(\mu)$	$\lambda_o(\mu)$	W(v)	$a_o(\mu)$	$\frac{a_o(\text{numer.})}{a_o(\text{analyt.})}$
23	16.67	4.0	0	0.55	0.55	0.55	-	0.729	-
25	"	"	"	0.38	0.68	"	v^1	0.622	-
28	"	3.0	"	0.5	0.5	0.5	-	0.844	-
32	"	"	"	0.4	0.7	"	v^1	0.869	-
31	"	"	0.40	0.47	0.53	"	"	1.701	1.031
33	"	1.0	"	0.4	0.7	"	"	3.674	1.067
13	"	2.0	"	"	"	"	"	3.499	1.016
30	"	3.0	"	"	"	"	"	3.465	1.006
4	"	4.0	"	"	"	"	"	3.455	1.003
34	"	1.0	"	"	"	0.55	"	4.051	1.122
35	"	2.0	"	"	"	"	"	3.687	1.021
36	"	3.0	"	"	"	"	"	3.643	1.009
37	"	4.0	"	"	"	"	"	3.627	1.004
26	12.00	3.0	"	"	"	0.5	"	2.495	1.007
6	16.67	"	0.54	"	"	"	"	4.019	1.004
7	"	4.0	"	"	"	"	v^0	4.045	1.002
1	"	"	"	"	"	0.55	"	4.050	1.004
2	"	"	"	"	"	"	v^1	4.209	1.003
3	"	"	"	"	"	"	v^2	4.428	1.003
8	"	"	"	"	"	0.5	v^1	4.010	1.002
10	"	"	"	"	1.0	"	"	4.477	1.002

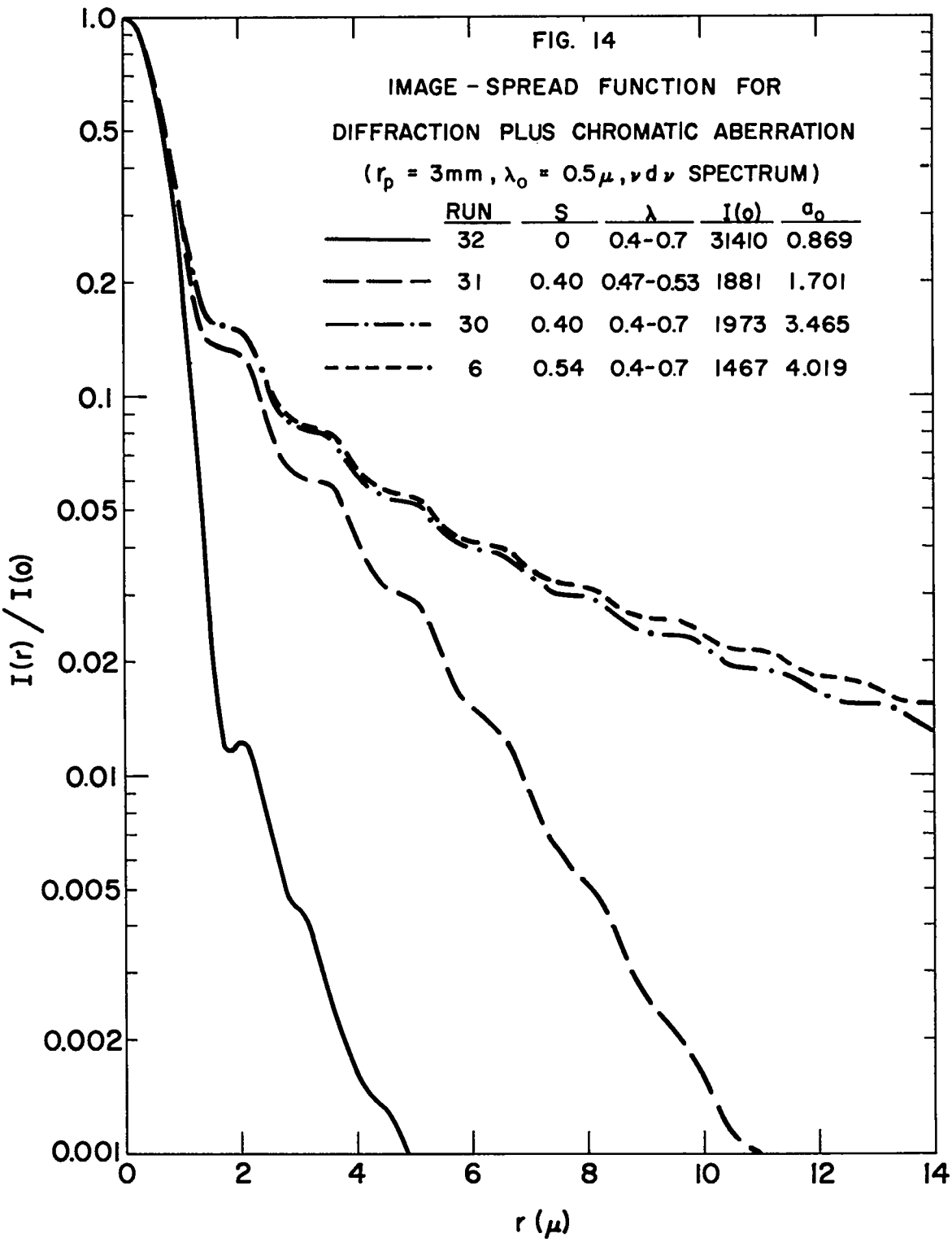
FIG. 14
IMAGE - SPREAD FUNCTION FOR
DIFFRACTION PLUS CHROMATIC ABERRATION
(r_p = 3mm, λ_0 = 0.5μ, $\nu d\nu$ SPECTRUM)
RUN S λ I(0) a_0
32 0 0.4-0.7 31410 0.869
31 0.40 0.47-0.53 1881 1.701
30 0.40 0.4-0.7 1973 3.465
6 0.54 0.4-0.7 1467 4.019
I(r) / I(0)
1.0
0.5
0.2
0.1
0.05
0.02
0.01
0.005
0.002
0.001
0
2
4
6
8
10
12
14
r (μ)

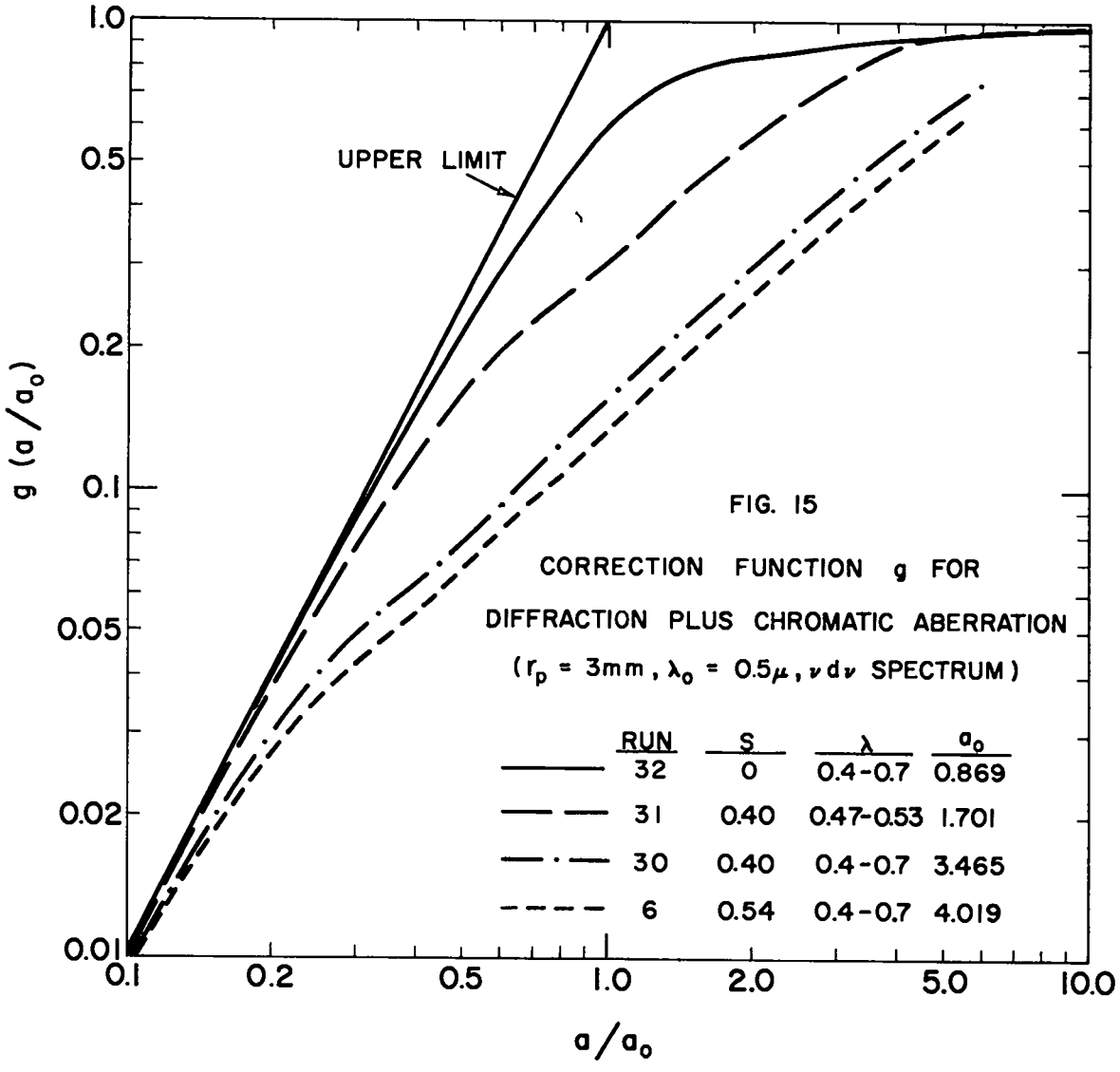
1.0
0.5
0.2
0.1
0.05
0.02
0.01
g (a/a0)
UPPER LIMIT
0.1
0.2
0.5
1.0
2.0
5.0
10.0
a/a0
FIG. 15
CORRECTION FUNCTION g FOR
DIFFRACTION PLUS CHROMATIC ABERRATION
(rp = 3mm, λ0 = 0.5μ, ν dν SPECTRUM)
RUN S λ a0
32 0 0.4-0.7 0.869
31 0.40 0.47-0.53 1.701
30 0.40 0.4-0.7 3.465
6 0.54 0.4-0.7 4.019

The calculated form of I(r) is shown in Fig. 14 for four of these cases [the quantity I(o) tabulated is the value of the integral in (64), in diopters$^2/\mu^4$]. Note the very strong central diffraction peak (cf. the remarks of pp. 50-51), whose shape out to $r \cong 1\mu$ is nearly independent of the dispersion and spectral range.

The corresponding functions $g(a/a_o)$ are shown in Fig. 15. The curves for runs 30 and 6 lie much lower than the "experimental" curves of Fig. 2. This is the result of the very long tails of the I(r) curves (compared with their slopes at small r), and is related to the very large values of $a_o/r_h \cong 5$ for these curves. (The reason for the differences among the g curves can also be seen from a different point of view: The spectrum of run 30 contains about four times the energy of the spectrum for run 31, but it is clear from Fig. 14 that this extra energy really contributes almost nothing to the eyedose, even for rather large source radii. This is completely allowed for at small $x = a/a_o$, where $g \propto x^2$, by the value of a_o being twice as great for case 30 as for 31. But for $x \cong 1$, g is more nearly proportional to the first power of x, and the larger value of a_o allows for only a factor two in energy; the remaining factor two shows up in the g curve for run 30 being about a factor two lower than for run 31.)

For small entrance pupils ($r_p < 2$mm), chromatic aberration is considerably reduced and the diffraction peak considerably widened. I(r) then shows no pronounced central peak (i.e., no large change in slope on a semi-log plot), and the curves are more like the upper two curves in

Fig. 15, even though a_o is still 3.5 to 4μ.

E. Effects of Age and Individual Variations

The analytical result (69) for a_o and the numerical results of Table III and Fig. 15 give the information required for the retinal-dose problem provided we have an optically perfect emmetropic eye of known focal length and dispersion. So far, we have used mostly the typical adult values f_o = 16mm and S = 0.40-0.54 diopter - μ^2. In this section, we consider in some detail the values which should be used to cover all likely cases of eyes which are optically perfect, but which have physical sizes different from the average, or which are ametropic and require correction with spectacle lenses.

We consider first emmetropic eyes, in which the natural refracting power and axial length of the eye are properly matched so as to provide an image of a distant object on the retina with zero (or relatively little) accommodation of the lens. In this case, the main question is the range of focal lengths which one must consider. As an extreme case we immediately think of children, whose small eyes have short focal lengths which produce smaller and (other things being equal) more intense retinal images. However, this does not mean that the thermal dose received by the retina of a child will be much larger than that of an adult. In the first place, children's eyes are really not much smaller than adults':[28,29]

AXIAL LENGTH OF EYE

Age	Ave (Range)	Relative size
0 yr	15 (13-17)	0.63 (0.54-0.71)
1	19	0.79
6	22	0.92
adult	24	1.00

Thus for children older than one year the effect could hardly be more than sixty percent in intensity. But more importantly, the smaller eyeball of the child probably means also a smaller entrance-pupil radius r_p, and therefore less light entering the eye. Indeed, geometrical intensity and diffraction and chromatic-aberration effects (for given S) all depend on r_p and f_o only through their ratio, so that to the extent that r_p/f_o is independent of eyeball size, so also is the retinal dose: In terms of the above mathematical analysis, it follows from (1) and (70) that $g(a/a_o)$ is independent of r_p and f_o (for given S), and from (7) that the eyedose is proportional to $(r_p/f_o)^2$.

Thus we will ignore children as a special case, so far as r_p/f_o is concerned, and consider only the maximum value of this ratio which is observed in adults. Extensive statistical studies have been made on the variation of refracting power and eyeball length.[22,23] In a study of 1000 eyes by Stenström,[22] the total refracting power of the unaccommodated eye was found to vary from 52.5 to 63.5 diopters, with a mean value of 58.13; only about one percent of the eyes had a power greater than 62.5

(f_o = 16mm). The pupillary radius under conditions of low luminence (10^{-6} millilamberts) varies from 3.2 to 4.5mm, depending on age, etc.[30] It seems likely that there is a certain degree of correlation between large pupil and large focal length; hence it should not be necessary to use the extremes of both large pupil and short focal length, and a reasonably conservative value for eyedose calculations on emmetropic eyes should be

$$r_p/f_o = 4.0/16.0 = 1/4 \ . \qquad (73)$$

The question of the value to be used for S was discussed in Sec. 4C in connection with Fig. 12. It was shown there that $S \cong 0.54$ for eyes with an unaccommodated power of 58 diopters; that emmetropic adult eyes do not have a power less than about 90 percent of this (children's eyes tend to have a higher power); that S should thus not be less than about $0.90 \cdot 0.54 = 0.49$; and that $S = 0.40$ should be quite a conservative value for all emmetropic eyes.

We consider now an ametropic eye whose refractive error has been corrected with a spectacle lens of power P_s placed a distance c in front of the vertex of the reduced eye (Fig. 16). For parallel light incident on the optical system consisting of spectacle lens plus reduced eye, we have the following relations:

$$p_e = c - q_s = c - f_s \ ,$$

$$\frac{f_e}{c - f_s} + \frac{f'_e}{q_e} = 1 ,$$

$$\frac{1}{q_e} = \frac{1}{f'_e} + \frac{f_e}{f'_e(f_s - c)} = \frac{f_e + f_s - c}{f'_e(f_s - c)} . \tag{74}$$

From similar triangles in Fig. 16 we find the ratio of entrance to exit pupil size to be

$$\frac{r_n}{r_x} = \frac{f_s}{f_s - c} = \frac{f'}{q_e} , \tag{75}$$

from which

$$f' = \frac{f'_e f_s}{f_e + f_s - c}$$

or

$$1/f \equiv P = P_e + P_s - c\, P_e P_s . \tag{76}$$

In the notation of (61)-(62),

$$S = \frac{1}{n'_o} \frac{dP}{d(\nu^2)} = n'_o \frac{dP'}{d(\nu^2)} = n'_o \frac{d(1/f')}{d(\nu^2)} \tag{77}$$

[cf. Eq. (47)], but f' there really represents the distance from exit pupil to plane of focus, so that in the present case we must calculate

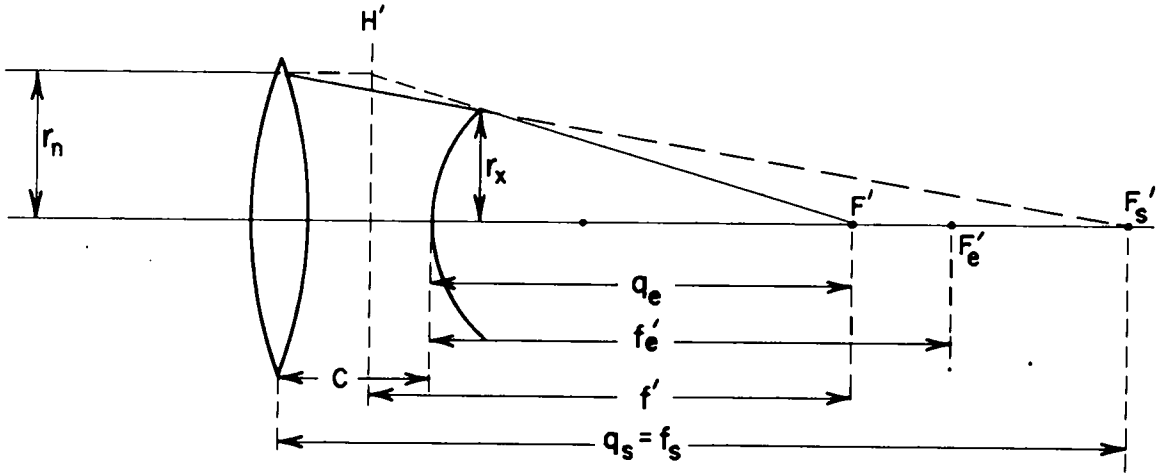

FIG. 16

REDUCED EYE WITH SPECTACLE LENS

S from

$$S = n_o' \frac{d(1/q_e)}{d\nu^2} . \tag{78}$$

Differentiating (74), using (47), and noting that

$$\Delta P_s = x\, P_s \Delta P_e / P_e ,$$

where x is the ratio of the dispersion $\Delta n/(n - 1)$ for spectacle glass to the dispersion of the reduced eye, one finds

$$S = \left\{ 1 + \frac{P_s/P_e}{1 - c\,P_s}\left[1 + n'\left(\frac{x}{1 - c\,P_s} - 1 \right)\right]\right\} \cdot \frac{1}{n'} \frac{d\,P_e}{d(\nu^2)} . \tag{79}$$

The ratio of this to the value S_n for a normal eye of power P_n is from (77)

$$\frac{S}{S_n} = \frac{P_e}{P_n}\left\{ 1 + \frac{P_s/P_e}{1 - c\,P_s}\left[1 + n'\left(\frac{x}{1 - c\,P_s} - 1 \right)\right]\right\} . \tag{80}$$

Ordinary eyeglasses are usually mounted about 12mm in front of the cornea* so that c (which is really the distance to the principal plane H′ of Fig. 3; cf. Figs. 6, 7) is about 0.014m. For contact lenses, $c \cong 0.002$m. In any case, the required value of

*Reference 22, Chap. 16. This makes c nearly equal to f_e so that $P \cong P_e$ from (76), and the size of the image on the retina is nearly the same as it would be for an emmetropic eye of power P_e.

$$\frac{P_s}{1 - c\,P_s} = \frac{1}{f_s - c}$$

is seen from (74) to be independent of c. We therefore rewrite (80) for the case of contact lenses (and make the approximation c = 0 in the term involving x; this always makes S too small). The dispersion of the ocular media has been shown to be greater than that of water, and the dispersion of extra-dense flint glasses is less than twice that of water,[31] so we shall use $x \cong 1.5$. Then

$$\frac{S}{S_n} \cong \frac{P_e}{P_n}\left\{1 + \frac{P_s}{P_e}\left(1 + \frac{n'}{2}\right)\right\} \quad . \tag{81}$$

The vast majority of eyes require corrections, at the cornea, of at most $P_s = \pm 10$ diopters, and these extreme values correspond respectively to $P_e \cong 58 \pm 5$ (i.e., an extremely hyperopic eye, requiring $P_s \sim +10$, is hyperopic because the eyeball is abnormally short, with which go small radii of curvature and high refractive powers; and vice versa).[22] Thus, taking $P_n = 58$,

$$\frac{S}{S_{58}} \cong \begin{cases} (63/58)(1 + 16.7/63) = 1.37 , & P_s = +10 , \\ (53/58)(1 - 16.7/53) = 0.62 , & P_s = -10 . \end{cases}$$

Thus the obvious effect on S due to the higher dispersion of glass [the factor in braces in (81)] is reinforced by the factor P_e/P_n which represents the effect of the different power of the eye itself, and the total

effect is appreciable. However, the important quantity for eyedose purposes is a_o, which from (69) is proportional to $f_o S^{1/2}$. Again, "f_o" is to be measured here by q_e/n'_o, the reciprocal of which is, from (74),

$$P_{eff} = n'_o/q_e = P_e + P_s/(1 - c\,P_s) \ .$$

Taking as before the value of P_s required at the cornea ($c \cong 0$), then P_{eff} is about 73 or 43 for $P_s = +10$ or -10, respectively, and

$$\frac{a_o}{a_{o_{58}}} = \frac{P_{58}}{P_{eff}}\left(\frac{S}{S_{58}}\right)^{1/2} \cong \begin{cases} 0.79 \cdot 1.17 = 0.92 \ , & P_s = +10 \ , \\ 1.35 \cdot 0.79 = 1.07 \ , & P_s = -10 \ . \end{cases}$$

Thus the change in S is more than offset by the change in distance from exit pupil to retina, and the total effect on a_o is small.

Another extreme case which can be considered is that of an aphakic eye (lens surgically removed), where the refracting power of the cornea ($P_e \cong 43$) is supplemented by a 12-diopter contact lens. Then

$$\frac{S}{S_{58}} = \frac{43}{58}\left\{1 + \frac{12}{43} \cdot \frac{5}{3}\right\} = 1.09 \ ,$$

$$\frac{a_o}{a_{o_{58}}} = \frac{58}{55}(1.09)^{1/2} = 1.10 \ .$$

The difference from the value for the normal eye is small and on the favorable side.

Thus use of (73) and S = 0.40 should be sufficiently conservative

to cover all eyes, with or without simple correcting lenses.

F. Other Aberrations

So far, we have considered only the effects of diffraction and chromatic aberration, and have assumed the eye to be otherwise perfect; that is, for a given wavelength, the amplitude and phase of the light converging on the retina have been assumed constant over the portion of an imaginary spherical surface which is bounded by the exit pupil and centered on the geometrical image point. The actual amplitude variations across the pupil are small, and in any case have relatively little effect on the shape of the diffraction pattern.[27] Phase variations, due to spherical aberration or more irregular defects, can however greatly modify the image pattern.*

The human eye appears to be largely corrected for spherical aberration, and it is commonly stated that in good eyes the effects of spherical aberration are negligible compared with those of chromatic aberration. In one sense this is true: experiments show that the power of some eyes varies as little as 0.1 to 0.2 diopters from the center of the pupil out to a radius of 2mm.[32] This is indeed small compared with the chromatic variation in power, which is two or three diopters over the visible region [Fig. 12 and Eq. (46)]. Of importance for present

*The effects of spherical aberration are illustrated in reference 24, plates 22 and 24. See also reference 14, pp. 476 f.

purposes, however, is the fact that a spherical aberration of only 0.1 diopter represents quite a large phase error: Taking the aberration-free corneal surface to be nearly spherical with radius R, then from Fig. 17, the extra distance which light travels in air when incident at a radius r from the optic axis (compared with the distance for r = 0) is

$$t_o \cong R - (R^2 - r^2)^{1/2} \cong r^2/2R$$

and

$$dt_o/dr = r/R \ .$$

For a slightly different cornea in which the power ($\propto R^{-1}$) varies, say, quadratically with r up to a maximum fractional difference $\Delta P/P$ at $r = r_p$,

$$\frac{dt}{dr} = \frac{r}{R}\left(1 \pm \frac{\Delta P}{P} \cdot \frac{r^2}{r_p^2}\right) ,$$

or

$$t = \frac{r^2}{2R} \pm \frac{\Delta P \ r^4}{4P \ R \ r_p^2} \ .$$

The maximum difference is [since $P = (n' - 1)/R$]

$$|t - t_o|_{max} = \frac{\Delta P \ r_p^2}{4(n' - 1)} \ . \qquad (82)$$

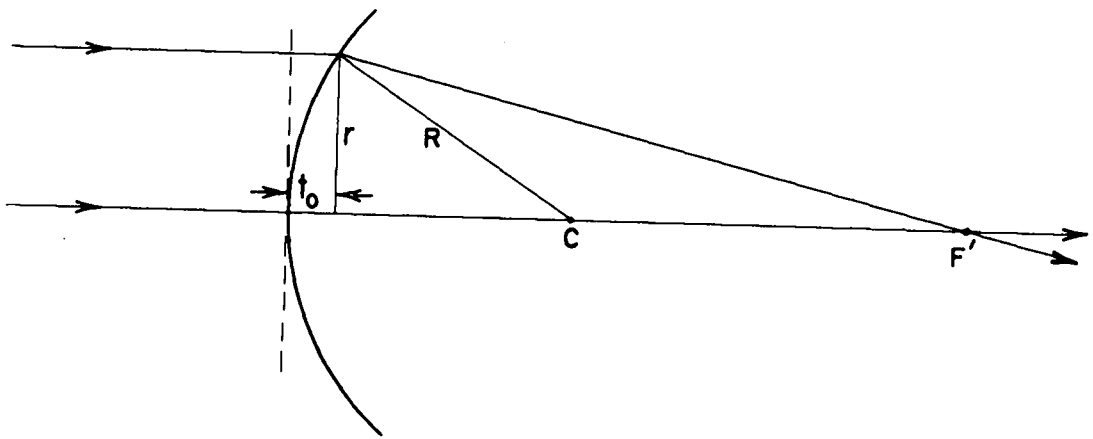

FIG. 17

MERIDIONAL RAYS for SPHERICAL INTERFACE

For even a 0.1 diopter difference in power between central and marginal rays at $r_p = 4$mm, this gives a maximum phase difference of about

$$\frac{(n' - 1)|t - t_o|_{max}}{\lambda} = \frac{0.1 \cdot 0.004 \cdot 4000}{4 \cdot 0.5} \cong 0.8 \quad \text{wavelength} \quad (83)$$

This estimate of phase error is confirmed by experiments measuring the detailed wave aberration[33] over the area of the pupil, which show irregular phase variations of at least ±1 to 2 wavelengths, and usually considerably more.[34] It would indeed be surprising if the eye -- a biological system, with variable-curvature surfaces in the lens -- did not show irregularities of this order [i.e., physical irregularities of $\pm 0.5\mu/(n' - 1) = \pm 1.5\mu$], when ordinary optical instruments may show wave aberrations as great as 40 or 50 wavelengths.[33]

The point of all this is that the phase variations, in effect, destroy to a considerable extent the coherency of the light reaching the vicinity of the geometrical focus. The strong central diffraction peak of Fig. 14 is thereby broadened and reduced in intensity to a greater or lesser extent. The quantitative intensity distribution in the vicinity of the paraxial focus can be computed in the case of pure spherical aberration,[35] but there is no point in going into details here because the calculations are not applicable for the irregular wave aberrations of the eye observed by Smirnov.

There are additional complications in calculating the intensity distribution on the retina of the real eye -- namely, scattered light.[36-38]

This scattering is the result of the fact that none of the parts of the eye -- cornea, lens, vitreous humor, and retina -- is homogeneous, but rather shows cellular and other structure on a scale of roughly 5 to 30 microns.[39] Experimental results (Fig. 11 and reference 36) appear to indicate that nearly half of the light entering the eye suffers large-angle scattering (greater than one half to one degree). If anything like this much large-angle scattering really exists, then there surely must be sufficient small-angle scattering to completely obliterate all diffraction structure in the retinal image.

Thus, between the gross refraction errors of the eye and the scattering due to fine structure, it seems highly probable that little or nothing remains of the central diffraction peak of the functions I(r) shown in Fig. 14. This means that the central intensity I(o) may really be a factor four or more lower than calculated on the basis of diffraction and chromatic aberration alone, and that a_o is therefore to be increased by a factor two or so. This gives

$$a_o = 7 \text{ to } 8\mu \,, \tag{84}$$

which is approximately the value (33) deduced from experiment.

The function g appropriate to this larger value of a_o is of course not like the functions shown in Fig. 15. In order to calculate the rough forms of I(r) and $g(a/a_o)$, there has been added to the RCØ code a feature by which a new function $I_{ave}(r)$ has been obtained by replacing I(r) with the value found by averaging I(r) over a circle of radius r_o centered at r:

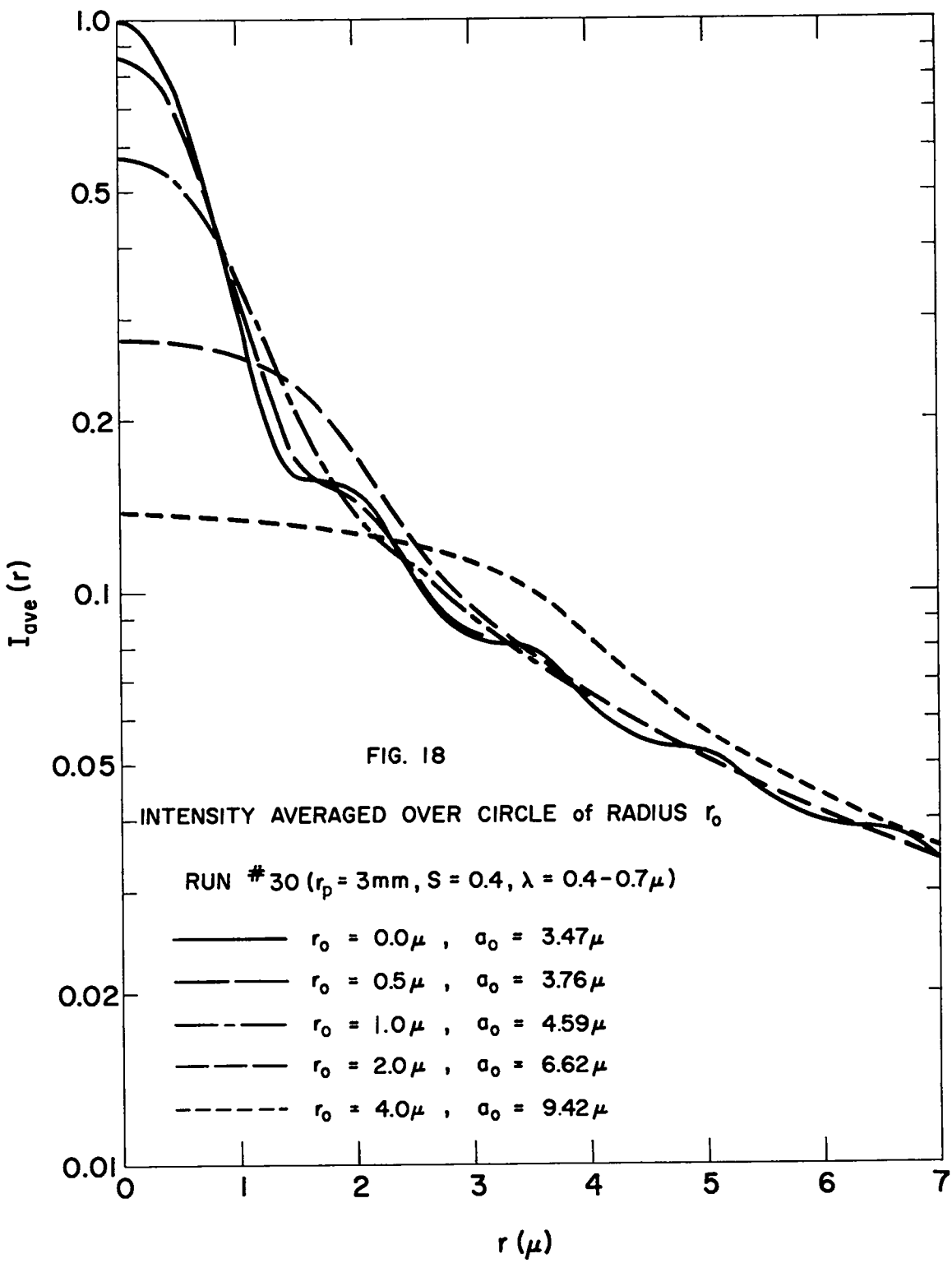
1.0
0.5
0.2
0.1
0.05
0.02
0.01
$I_{ave}(r)$
0
1
2
3
4
5
6
7
r (μ)
INTENSITY AVERAGED OVER CIRCLE of RADIUS r_o
RUN # 30 (r_p = 3mm, S = 0.4, λ = 0.4-0.7μ)
r_o = 0.0μ , a_o = 3.47μ
r_o = 0.5μ , a_o = 3.76μ
r_o = 1.0μ , a_o = 4.59μ
r_o = 2.0μ , a_o = 6.62μ
r_o = 4.0μ , a_o = 9.42μ

FIG. 18

$$I_{ave}(r) = \frac{\int_0^{r_o} \int_0^{2\pi} I(\vec{r}' - \vec{r}) \cdot |\vec{r}' - \vec{r}| \, d\varphi \, d|\vec{r}' - \vec{r}|}{\int_0^{r_o} \int_0^{2\pi} |\vec{r}' - \vec{r}| \, d\varphi \, d|\vec{r}' - \vec{r}|} \cdot \quad (85)$$

Some results for $I_{ave}(r)$ are shown in Fig. 18 and, renormalized to $I_{ave}(0) = 1$, in Fig. 19. The corresponding functions $g_{ave}(a/a_o)$ are shown in Fig. 20; these functions of course rise to unity appreciably sooner than does the unaveraged one (because of the larger value of a_o).

It is suggested that the curves for $r_o = 2.0$ are the most appropriate: This value of r_o is sufficient to wipe out the diffraction peak and about double the value of a_o, and the resulting curves are very similar both to those of Fig. 2 and to the curves calculated by Mayer, et al.[3]

Results for other values of r_p, S, and λ_o are summarized in Table IV.

5. Summary and Conclusions

We have assumed a spherical source of radius $R = R(t)$ which has a "brightness" in the visible region $B = B(t)$ watts/cm^2-ster, and which is viewed from a distance D by an eye of focal length f_o (referred to air) for the wavelength of focus λ_o ($\cong$0.56μ or 0.5μ for daylight or nighttime viewing, respectively[18]). If the eye were optically perfect, it would form on the retina a geometrical image of radius

$$a = R f_o/D \quad (86)$$

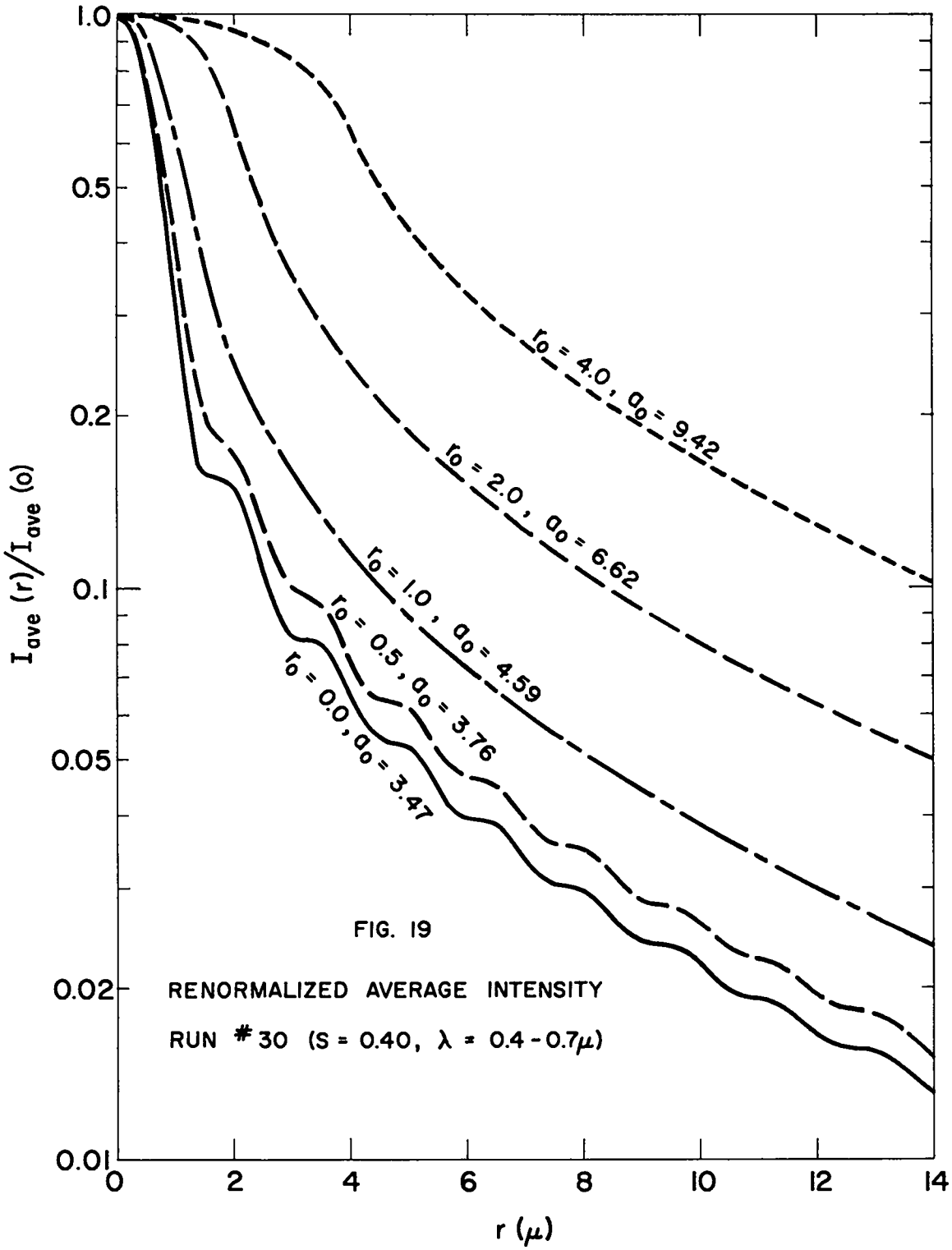

FIG. 19

RENORMALIZED AVERAGE INTENSITY

RUN # 30 (S = 0.40, λ = 0.4 - 0.7μ)

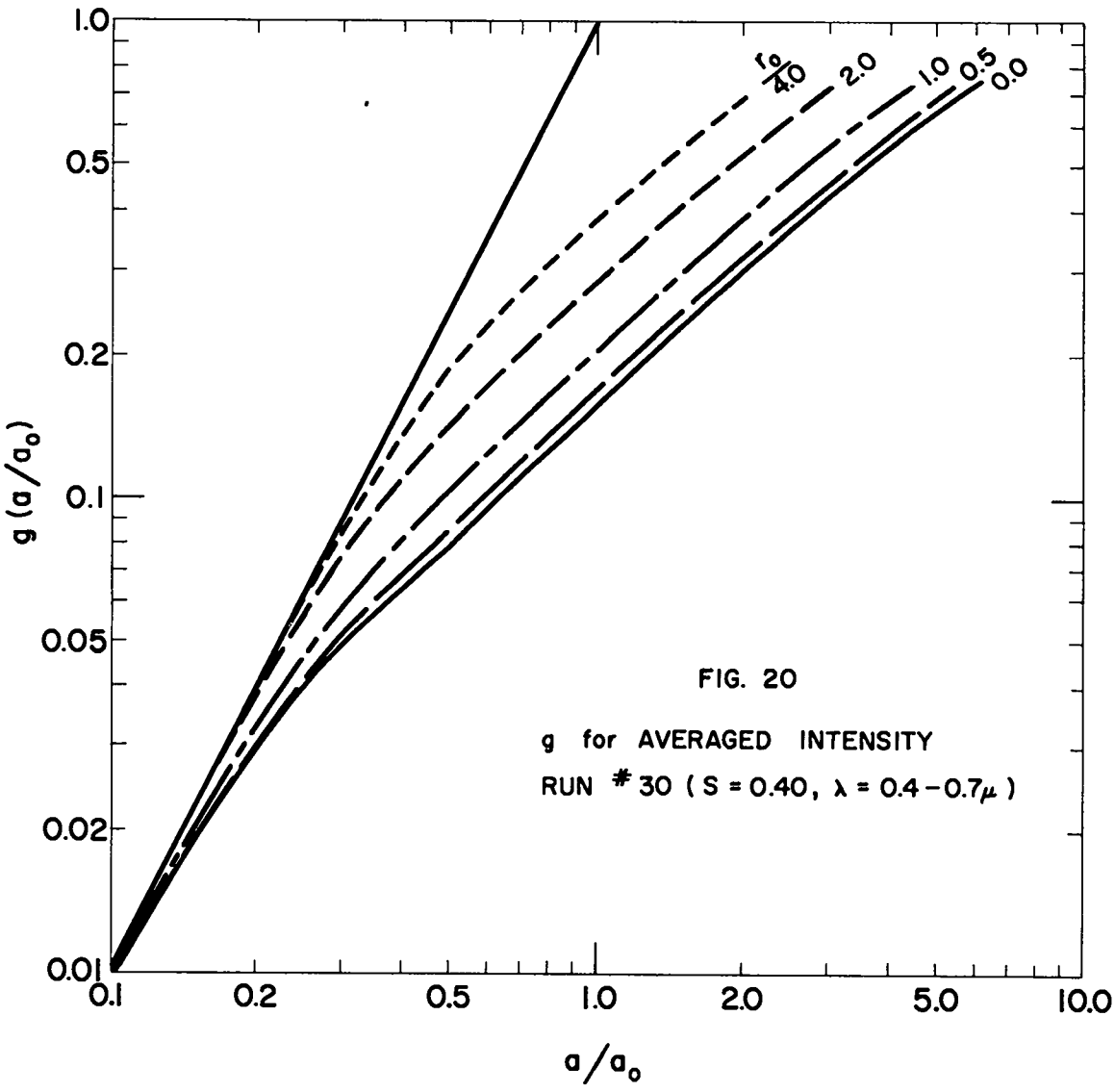

FIG. 20

g for AVERAGED INTENSITY

RUN # 30 (S = 0.40, λ = 0.4 − 0.7μ)

of uniform intensity I_{geom}. Because of diffraction, optical aberrations, and scattering within the eye, the image actually extends over an area greater than $\pi\ a^2$, and the maximum intensity of the image is reduced by some factor, Eq. (6),

$$g = g(a/a_o) \equiv I_{max}/I_{geom} \leq 1 \ , \tag{87}$$

where a_o is an effective point-source image radius (such that if all the energy in the image were spread uniformly over a circle of radius a_o, the intensity would be equal to I_{max}).

It was shown in Sec. 2 that the peak time-integrated retinal dose, Eq. (7), is

$$\text{Retinal dose} \equiv \int I_{max}\ dt$$

$$= \frac{\pi\ T\ r_p^2}{4.18 f_o^2} \int g\ B\ dt\ \text{cal/cm}^2 \ , \tag{88}$$

where r_p is the radius of the entrance pupil of the eye and the integral extends over $0 \leq t \leq \sim 0.15$sec. The value of r_p/f_o was shown, Eq. (73), to be no greater than 1/4 under nighttime conditions, so that

$$\text{Retinal dose} = \frac{T}{21} \int_0^{0.15} g(a(t)/a_o)B(t)\ dt \ . \tag{89}$$

It was shown in Sec. 4D that for unresolved images the contribution to

TABLE IV

VALUES OF a_o AND g(1) FOR I_{ave}

(f_o = 16.67mm, $\nu\, d\nu$ spectrum from 0.4 to 0.7μ)

Run no.	r_p(mm)	S	λ_o(μ)	a_o(μ)				g(1)			
				$r_o = 0$	$r_o = 1$	$r_o = 2$	$r_o = 4$	$r_o = 0$	$r_o = 1$	$r_o = 2$	$r_o = 4$
32	3.0	0	0.5	0.87	1.21	2.16	4.14	0.593	0.628	0.748	0.839
33	1.0	0.40	"	3.67	3.81	4.21	5.74	0.454	0.465	0.483	0.567
13	2.0	"	"	3.50	4.01	5.42	7.79	0.232	0.263	0.341	0.456
30	3.0	"	"	3.47	4.59	6.62	9.42	0.157	0.206	0.287	0.387
4	4.0	"	"	3.46	5.34	7.57	10.80	0.119	0.182	0.250	0.341
34	1.0	"	0.55	4.05	4.18	4.57	6.06	0.442	0.449	0.466	0.538
35	2.0	"	"	3.69	4.14	5.42	7.87	0.238	0.264	0.333	0.444
36	3.0	"	"	3.64	4.63	6.67	9.47	0.160	0.206	0.284	0.379
37	4.0	"	"	3.63	5.31	7.57	10.85	0.124	0.179	0.247	0.335
6	3.0	0.54	0.5	4.02	5.33	7.66	10.87	0.136	0.179	0.249	0.339
8	4.0	"	"	4.01	6.20	8.77	12.49	0.103	0.157	0.217	0.299
2	4.0	"	0.55	4.21	6.16	8.77	12.52	0.107	0.155	0.215	0.294

I_{max} comes mainly from light with wavelengths near λ_o; T is then the transmission of the optical path between source and absorbing layer of the retina (pigmented epithelium) at the wavelength λ_o. For resolved sources, all wavelengths contribute, and T is then an appropriately-weighted average transmission. Experiments (Fig. 11 and reference 36) indicate the total transmission of the eye at λ_o = 0.5 to 0.55μ to be about 0.75-0.80, and the transmission of unscattered light to be about 0.35-0.40. However, there is some uncertainty in the validity of these numbers, and to be conservative we shall take the eye transmission to be 1.0; T then represents the transmission of the air between source and eye. B may conveniently be taken as the energy lying in the spectral region λ = 0.38 to 0.68μ, as this is the range of sensitivity of the film usually used in measuring B experimentally. (The infrared energy transmitted by the eye -- an additional 20 percent or so for the $\sim\nu\ d\nu$ spectrum of high-altitude explosions at times pertinent to the eyeburn problem -- is largely offset by the fact that the short-wavelength cut-off of air and eye is somewhat greater than 0.38μ.)

In any case, if the light from the source covers a frequency range $\nu_1 \leq \nu \equiv \lambda^{-1} \leq \nu_2$ with a distribution $W(\nu)\ d\nu$, and if one considers the eye to be optically perfect except for chromatic aberration (and diffraction), then the effective radius a_o was shown to be given by Eq. (69):

$$a_o \cong \frac{f_o}{\pi}\left\{\frac{S}{W(\nu_o)}\int_{\nu_1}^{\nu_2} W(\nu)\ d\nu\right\}^{1/2}$$

$$\cong \frac{f_o}{\pi}\left\{S(\nu_2 - \nu_1)\right\}^{1/2} . \qquad (90)$$

Here S is a measure of the chromatic aberration of the eye (of refractive index n′) at λ_o:

$$S \equiv \left[\frac{1}{n'}\frac{d(1/f)}{d(\nu^2)}\right]_{\lambda_o} ; \qquad (91)$$

for $f \cong 0.016$ meters and ν in microns^{-1}, it was shown in Sec. 4D to have a value probably about 0.54 and almost certainly greater than 0.40 diopter - μ^2. Using f_o = 16mm, S = 0.40, $\lambda_o = 0.5\mu$, and a $\nu\, d\nu$ spectrum one obtains

$$a_o \cong \frac{16 \cdot 10^3}{\pi}\left\{\frac{0.40 \cdot 10^{-6}}{2} \cdot \frac{1}{2}\left(\frac{1}{0.38^2} - \frac{1}{0.68^2}\right)\right\}^{1/2}$$

$$= 3.51\mu . \qquad (92)$$

Under the conditions assumed for this value of a_o, the calculated point-source image-spread function I(r) is the curve marked "r_o = 0.0" in Fig. 19 (that curve was actually calculated for a spectrum from λ = 0.4 to 0.7μ, but the difference is negligible), and the corresponding correction function g is the lowest curve shown in Fig. 21. For use in machine calculations, g can be represented conservatively by the analytic function

$$g_1(x) \approx \min[0.17x, x^2/(1 + x + x^2)] , \qquad x = a/a_o , \tag{93}$$

which is also shown in the figure.

For a conservative calculation, the retinal dose should be evaluated from (89) using the function $g = g_1$ and a value $a_o = 3.5\mu$. The result should be an overestimate for even the best of eyes, regardless of age, sex, and whether or not the individual is wearing ordinary spectacles or contact lenses.

Because of aberrations and scattering within the eye, it is highly probable that the point-source image-spread function of even the best eyes looks more like the curve marked "$r_o = 2.0$" in Fig. 19. This means that it is <u>probably</u> legitimate to use

$$a_o \cong 7\mu , \tag{94}$$

a value which is more in accord with the experiments mentioned in Sec. 3. However, the corresponding function g(x), Fig. 21, lies appreciably higher than the curve appropriate to $a_o = 3.5$. A reasonable analytic function is

$$g_2(x) = x^2/(1 + x^2) , \qquad x = a/a_o . \tag{95}$$

As may be seen from Table IV, this function should always be used in preference to g_1 in the case of small r_p (daytime viewing).

For conditions under which x is always less than about 0.2 or always

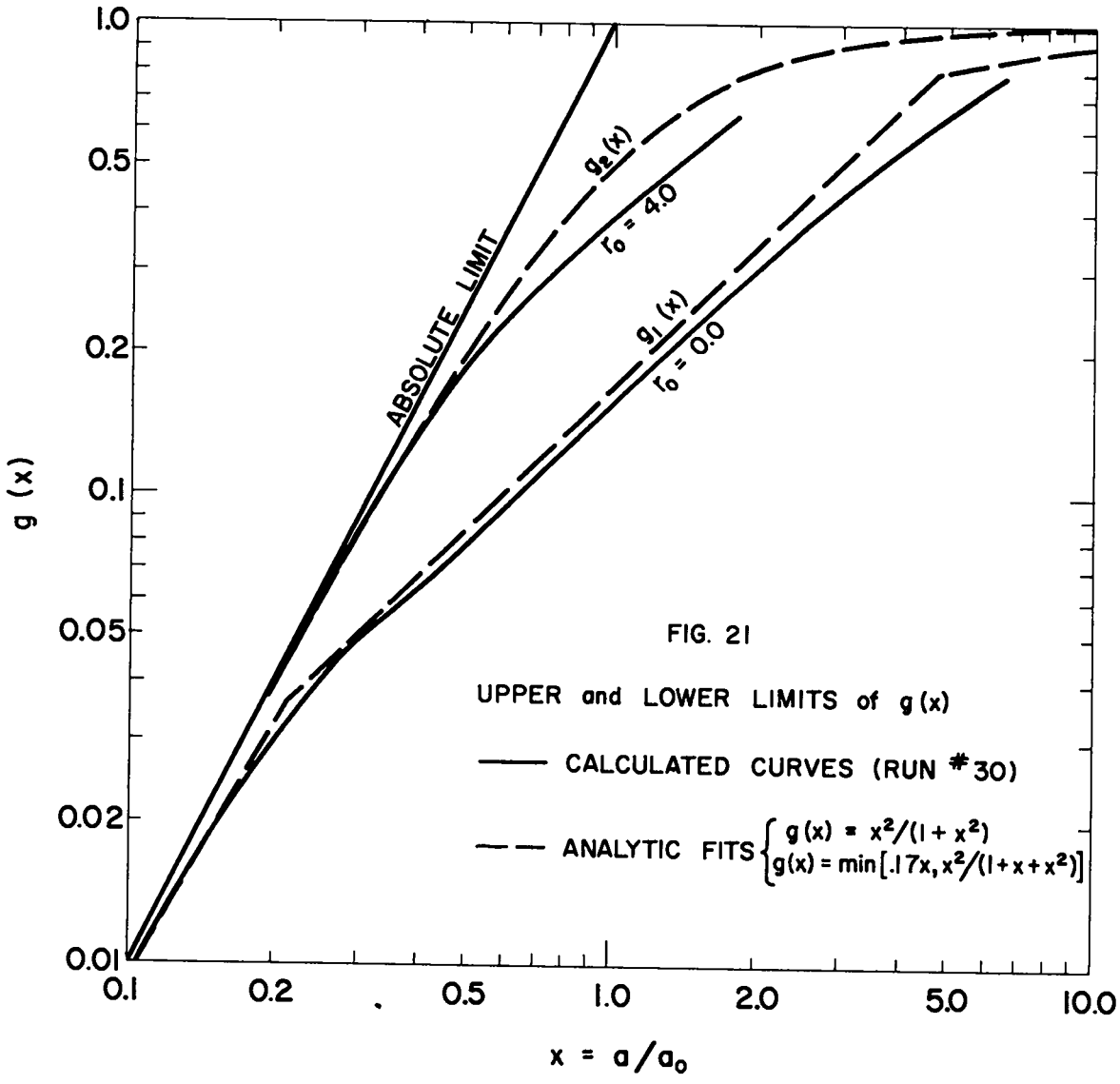
1.0
0.5
0.2
0.1
0.05
0.02
0.01
g (x)
0.1
0.2
0.5
1.0
2.0
5.0
10.0
x = a/a0
ABSOLUTE LIMIT
g2(x)
r0 = 4.0
g1(x)
r0 = 0.0
FIG. 21
UPPER and LOWER LIMITS of g(x)
CALCULATED CURVES (RUN #30)
ANALYTIC FITS
g(x) = x²/(1 + x²)
g(x) = min[.17x, x²/(1+x+x²)]

greater than about five during times which contribute to the eyedose, it makes little difference whether one uses g_1 or g_2. However, if the major contribution comes during the interval between 0.2 and 5, then the fact that $g_2 > g_1$ partially offsets the reduction in calculated dose due to the larger value of a_o. Moreover, the retinal-damage threshold dose could be somewhat lower with the large a_o than with the small value: The threshold should be that pertinent to a larger spot radius for large a_o than for small, and the former threshold could be lower because of less-effective sideward heat conduction in the retina. Such a lower threshold would also tend to offset the advantages of using a larger value of a_o.

Consequently, one may wish to calculate both ways: (1) use g_1 with $a_o = 3.5\mu$, (2) use g_2 with $a_o \cong 7\mu$, using in each case a threshold appropriate to a spot of radius about $(a^2 + a_o^2)^{1/2}$ with a the geometrical radius at the appropriate time, and see whether either calculated retinal dose is greater than the corresponding threshold. (In practice, it is likely that the difference between the two estimates will be small compared with the necessary margin of safety.)

6. Example

As a specific example of the calculation of retinal dose for a high-altitude explosion, we consider a hypothetical explosion in vacuum (with a yield of about a megaton), whose radius, temperature, and brightness histories are those shown in Fig. 22. (These curves were calculated with

a computer code RCH,[40] which gives only a smeared-out brightness at early times, using fictitious but realistic values of the input parameters.) The time-integrated radiated energy in the visible,

$$\int 4\pi^2 R^2 B \, dt \ ,$$

is $1.4 \cdot 10^{10}$ joules or $3.4 \cdot 10^{-3}$ ktons.

The geometrical radius of the retinal image depends from (86) on the distance of the observer from the source, and it is convenient to define a radius R_o which is the analogue of a_o projected into the plane of the source:

$$\frac{a}{a_o} = \frac{R\, f_o}{a_o D} \equiv \frac{R}{R_o} \ . \qquad (96)$$

[It should be noted from (90) that a_o is proportional to f_o, and so the same value of f_o should be used here as in the calculation of a_o -- namely 16mm.] The calculated eyedose depends on a_o and D only through their product, and so the value of the retinal dose can be found for most any a_o or D of interest by evaluating (89) for several values of this product, or equivalently of R_o.

Taking the values

$$a_o D = 1000, 2000, 4000, 8000 \mu\text{-km}$$

or

$$R_o = 62.5, 125, 250, 500 \quad \text{meters} \ ,$$

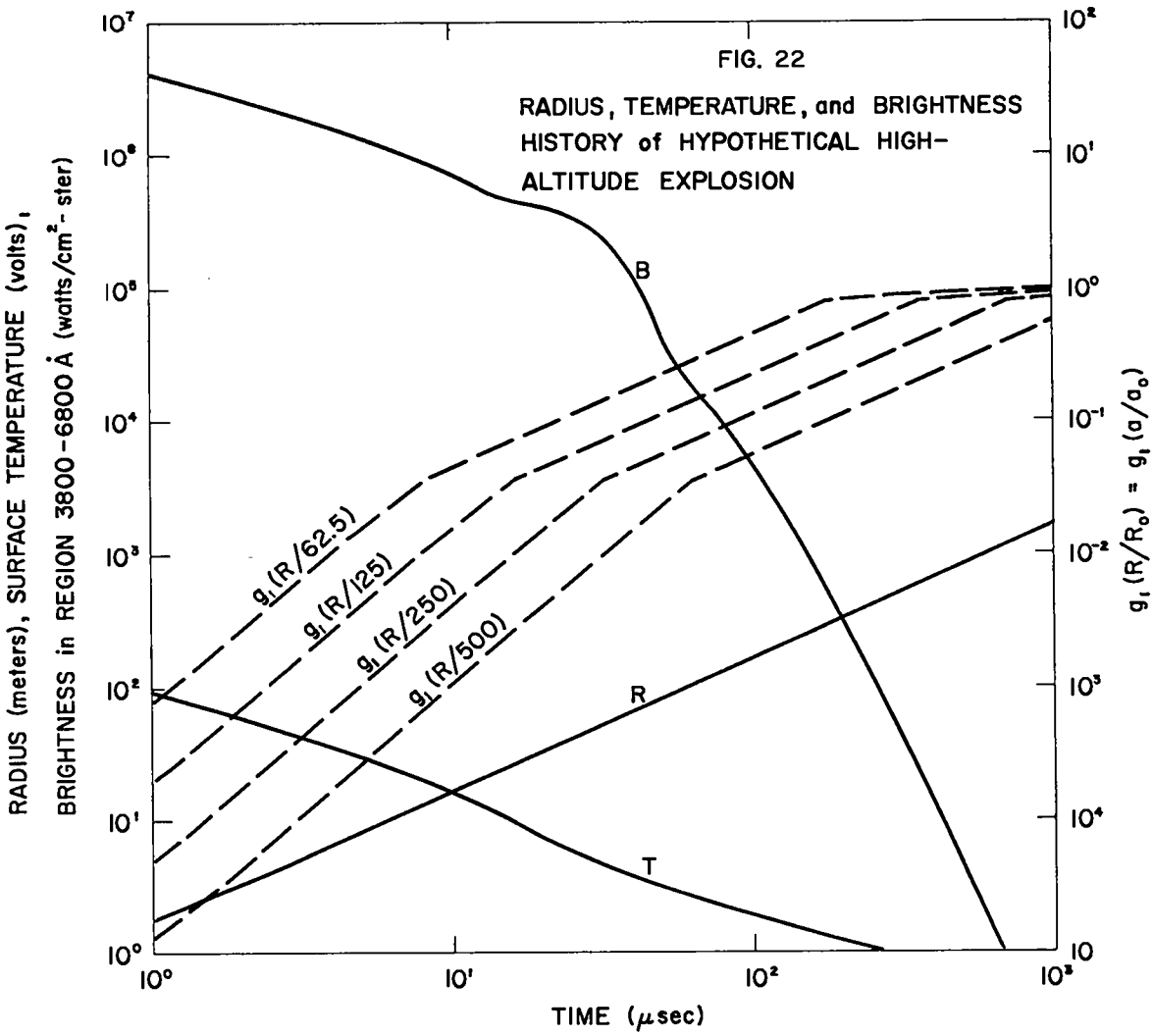

FIG. 22

RADIUS, TEMPERATURE, and BRIGHTNESS HISTORY of HYPOTHETICAL HIGH-ALTITUDE EXPLOSION

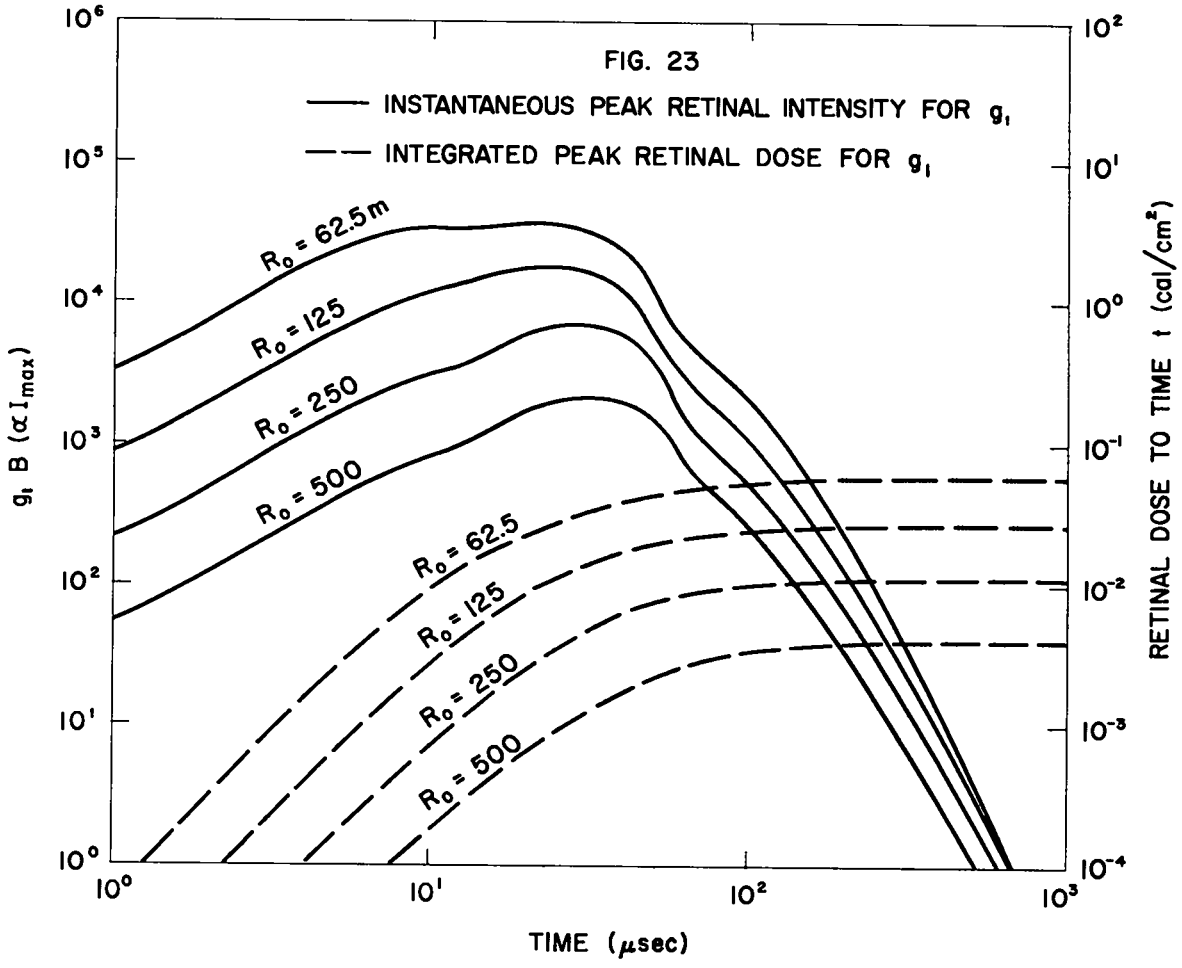
FIG. 23
INSTANTANEOUS PEAK RETINAL INTENSITY FOR g_1
INTEGRATED PEAK RETINAL DOSE FOR g_1
R_0 = 62.5m
R_0 = 125
R_0 = 250
R_0 = 500
R_0 = 62.5
R_0 = 125
R_0 = 250
R_0 = 500
g_1 B (αI_{max})
RETINAL DOSE TO TIME t (cal/cm²)
TIME (μsec)
10^6
10^5
10^4
10^3
10^2
10^1
10^0
10^2
10^1
10^0
10^{-1}
10^{-2}
10^{-3}
10^{-4}
10^0
10^1
10^2
10^3

and using the form g_1 given by (93), the four correction functions have the time dependence shown in Fig. 22, and the corresponding four products $g_1 B$ are as shown in Fig. 23. The accumulated retinal dose to time t for g_1 and each of the four values of R_o is also shown in Fig. 23. The figure shows that the retinal dose is delivered over a time interval of about 200μsec, but that delivery near the maximum rate occurs during an interval of only about 40μsec.

The four final values of the retinal dose for g_1, together with values for smaller R_o and similar results using g_2 instead of g_1 (the whole calculation being done by the code RCH), have been used to plot the nighttime curves of Fig. 24. For a slant range D of 1000km, these results indicate that under the conservative assumption $a_o = 3.5\mu$ the retinal dose (using the curve for g_1) is about

$$0.013T \quad \text{cal/cm}^2 ,$$

and that under the probably valid but less conservative assumption $a_o = 7\mu$ the retinal dose (using the curve for g_2) is about

$$0.007T \quad \text{cal/cm}^2 .$$

The threshold value for retinal burns in rabbits has been extensively investigated by Ham, et al.,[41,42] and a summary of their results for different exposure times and image sizes is shown in Fig. 25; the threshold appears to be about 0.1 to 0.2cal/cm^2 for exposure times of 10 to 100μsec and image radii of a few hundred microns. Since the threshold

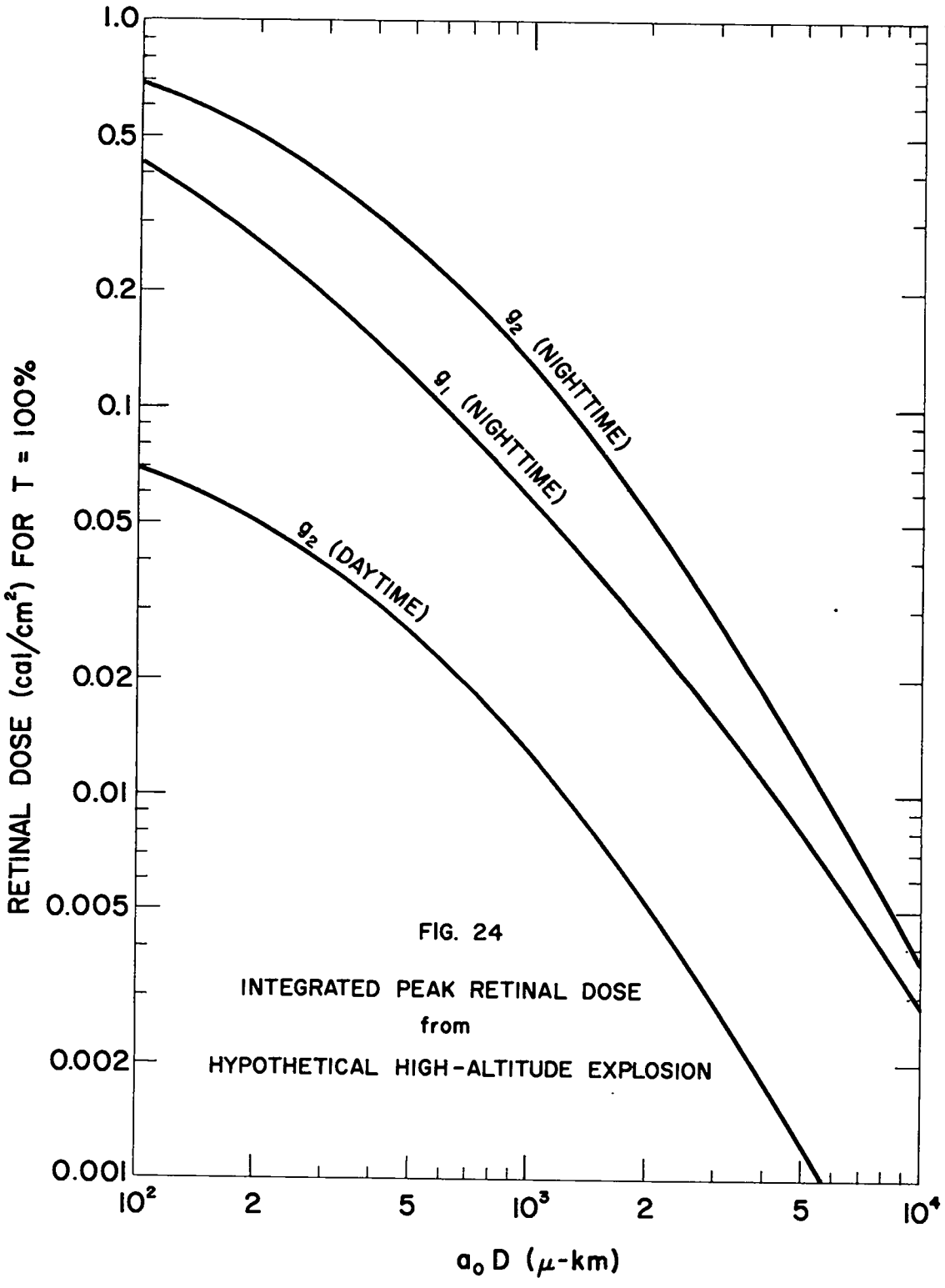

FIG. 24

INTEGRATED PEAK RETINAL DOSE
from
HYPOTHETICAL HIGH-ALTITUDE EXPLOSION

for radii of a few microns is if anything larger than this because of effects of heat conduction, the commonly used safe value 0.05cal/cm^2 for humans is probably conservative. Using this value and unit air transmission, Fig. 24 indicates no eyeburn danger down to a slant range of

$$\frac{1150}{3.5} = 330\text{km}$$

on the conservative basis, and a slant range of

$$\frac{2100}{7} = 300\text{km}$$

on the less-conservative basis. (The reason for the small difference between these two results is that the dose is here delivered at $a \cong a_o$, and one is approaching conditions under which the source is resolved and the retinal dose therefore independent of a_o.)

The above conclusions all apply to viewing under nighttime conditions. For an explosion during daylight hours (sky brightness $\cong$ 2 lamberts[43]), the radius of the pupil of the eye is only about 1mm instead of 4.[30] Calculations with the RCØ code show (cf. Table IV for $\lambda_o = 0.55$) that in this case one should use $a_o = 4\text{-}5\mu$ and the function g_2. The retinal dose (88) is therefore reduced about a factor 16 below the nighttime g_2 curve shown in Fig. 24. To be a little more conservative, the daytime curve has been drawn down a factor only 10, corresponding to $r_p = 1.26$mm. The minimum safe slant range is reduced to $200/a_o = 40\text{-}50$km.

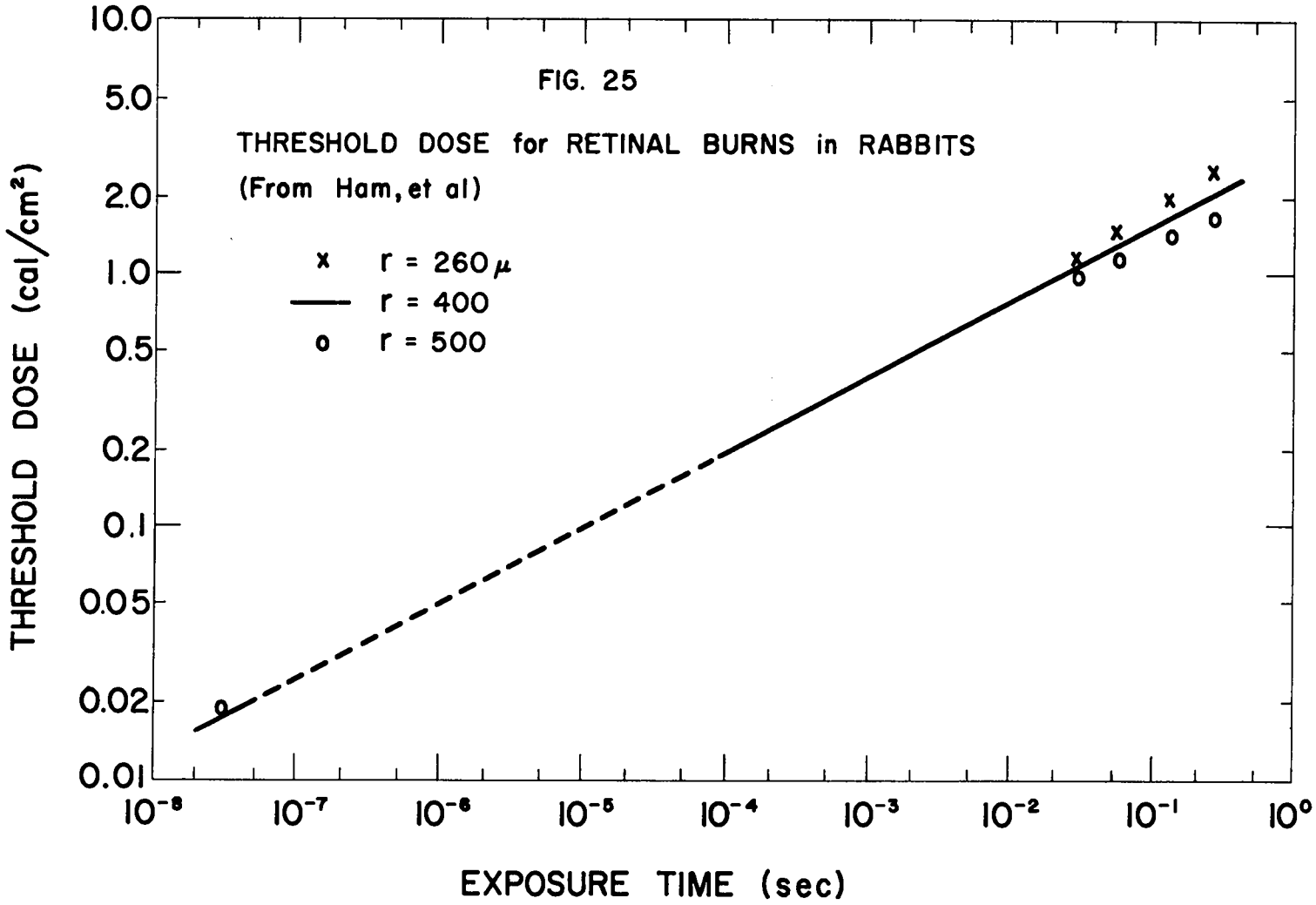
FIG. 25
THRESHOLD DOSE for RETINAL BURNS in RABBITS
(From Ham, et al)
x r = 260 μ
r = 400
o r = 500
THRESHOLD DOSE (cal/cm²)
10.0
5.0
2.0
1.0
0.5
0.2
0.1
0.05
0.02
0.01
10⁻⁸ 10⁻⁷ 10⁻⁶ 10⁻⁵ 10⁻⁴ 10⁻³ 10⁻² 10⁻¹ 10⁰
EXPOSURE TIME (sec)

On the other hand, if the explosion is viewed through binoculars or a telescope (with exit pupil no smaller than the entrance pupil of the eye), then the geometrical intensity of the retinal image is unchanged but the radius a of the geometrical image is increased by the magnification M of the instrument. Neglecting additional aberrations added by the instrument, the retinal dose will be the same (except for atmospheric transmission) as though the observer were only a distance D/M from the source, and can be found from the curves of Fig. 24 by using appropriately smaller values of the abscissa. Thus using 7-power glasses, the minimum safe slant range would be about 2100km at night and 400km in the daytime (for unit atmospheric transmission).

Appendix

In the treatment of chromatic aberration given in Sec. 4D, the reduced eye of Fig. 8 was used in Sec. 4C to establish the relation

$$S \equiv -\frac{dP_s}{d(\nu^2)} = n' \frac{dP'}{d(\nu^2)} = -\frac{n'}{f'^2}\frac{df'}{d(\nu^2)} , \qquad \text{(A-1)}$$

which was used in Eq. (62) to express the chromatic change in focal plane df' of an eye with fixed accommodation in terms of the measured power dP_s of a supplementary lens at the cornea required to shift the focal plane back to its original position. We will here show that this relation is correct for the more complicated eye of Fig. 6.

Let the focal lengths of supplementary lens, cornea, and crystalline lens be respectively f_s, f_c, f_ℓ when immersed in air, and let the distance between cornea and eye lens (assumed optically thin) be b (Fig. A-1). Then for parallel incident light, use of (36) twice gives

$$p_c = -q_s = -f_s ,$$

$$\frac{1}{q_c} = \frac{1}{f'_c} - \frac{f_c}{f'_c p_c} = \frac{f_s + f_c}{f'_c f_s} ,$$

$$p_\ell = b - q_c ,$$

$$\frac{1}{q_\ell} = \frac{1}{f'_\ell} - \frac{1}{p_\ell} = \frac{1}{f'_\ell} - \frac{f_s + f_c}{b(f_s + f_c) - f'_c f_s} ,$$

or

$$\frac{1}{q_\ell} = P'_\ell + \frac{P_s + P_c}{n' - b(P_s + P_c)}$$

$$= \frac{n'P'_\ell + (1 - b\,P'_\ell)(P_s + P_c)}{n' - b(P_s + P_c)} \,. \qquad \text{(A-2)}$$

From similar triangles

$$\frac{r_n}{r_x} = \frac{f'_{sc}}{f'_{sc} - b} = \frac{f'}{q_\ell} \,, \qquad \text{(A-3)}$$

so that since [cf. Eq. (76) for the case c = 0]

$$\frac{1}{f'_{sc}} = \frac{1}{n'f_{sc}} = \frac{1}{n'} (P_s + P_c) \,, \qquad \text{(A-4)}$$

then

$$f' = \frac{n'q_\ell}{n' - b(P_s + P_c)} = \frac{n'}{n'P'_\ell + (1 - b\,P'_\ell)(P_s + P_c)} \,. \qquad \text{(A-5)}$$

In the reduced eye, f′ is the same as the object distance, and df′ is therefore the shift in focal plane due to a change in wavelength. In the present case, however, the principal plane H′ may also shift with wavelength changes, and the true shift in focal plane [which is what is really meant by df′ in (51)] is given by calculating dq_ℓ. Differentiation of (A-2) gives

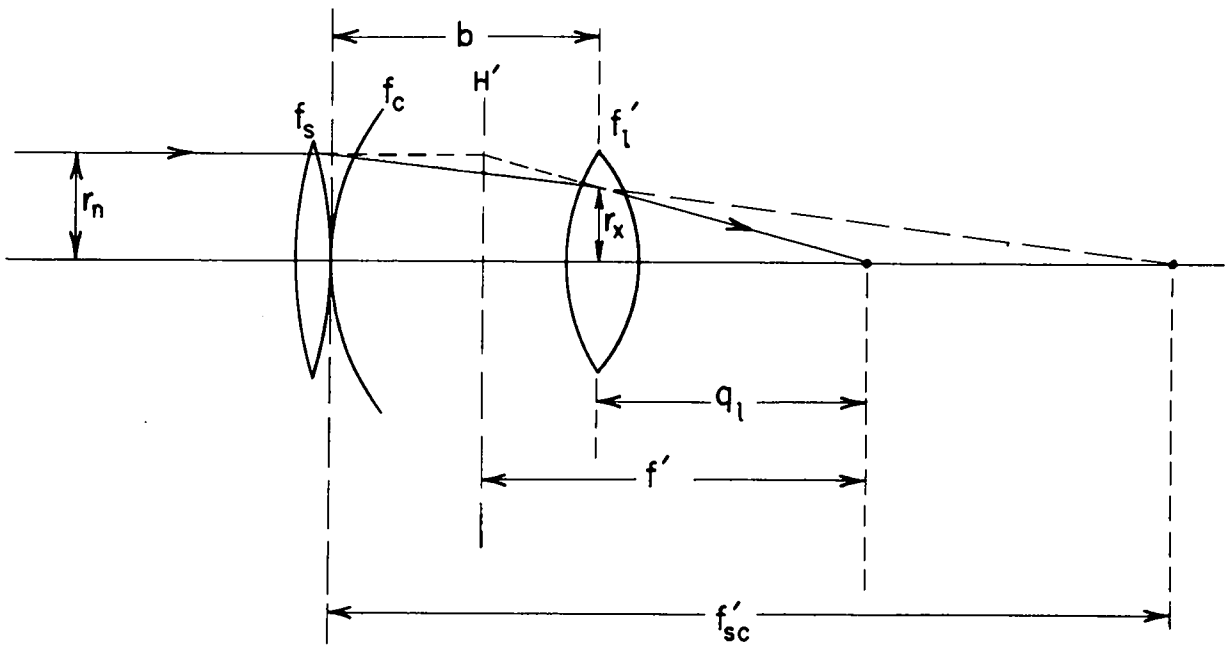

FIG. A-1

SCHEMATIC EYE WITH SUPPLEMENTARY LENS

$$-dq_{\ell} = \frac{n'dP_s + n'dP_c - (P_s + P_c)dn' + [n' - b(P_s + P_c)]^2 dP'_{\ell}}{[n'P'_{\ell} + (1 - b\,P'_{\ell})(P_s + P_c)]^2} .$$

From (45),

$$dn' = \frac{n' - 1}{P_c}\, dP_c ,$$

so that using also (A-5) we may write

$$-\frac{n'^2}{f'^2}\, dq_{\ell} = n'dP_s + [1 - (n' - 1)P_s/P_c]dP_c + [n' - b(P_s + P_c)]^2 dP'_{\ell} . \qquad (A\text{-}6)$$

The significance of this relation for the experiments in question is the following: The accommodation of the eye is fixed (presumably relaxed), and a distant object of wavelength λ_o is brought into focus by means of a supplementary lens of power P_s. (For an emmetropic eye, $P_s = 0.$) The wavelength of the object is now changed. Due to the changes in indices of refraction of the eye, the powers of cornea and lens (the latter referred to an external medium of index n') change by amounts dP_c and dP'_{ℓ}. If the power of the supplementary lens is unchanged, then the focal plane of the eye shifts by an amount dq_{ℓ}, given from (A-6) by

$$-\frac{n'^2}{f'^2}\, dq_{\ell} = [1 - (n' - 1)P_s/P_c]dP_c + [n' - b(P_s + P_c)]^2 dP'_{\ell} . \qquad (A\text{-}7)$$

In the experiments, P_s is then altered by an amount dP_s such as to bring

the eye back in focus, i.e., such as to make the right-hand side of (A-6) equal to zero. The required value of $n'dP_s$ is thus the negative of the right-hand side of (A-7), and the chromatic shift dq_l in focal plane of the eye is related to the measured power dP_s required to re-correct the eye by

$$\frac{n'^2}{f'^2}\, dq_l = n'dP_s \,, \tag{A-8}$$

which verifies the relation (A-1).

References

1. G. Westheimer, J. Opt. Soc. Amer. 53, 86 (1963).
2. G. A. Fry, J. Opt. Soc. Amer. 53, 94 (1963).
3. H. L. Mayer, R. M. Frank, and F. Richey, "Point Image Spread Function for Nuclear Eyeburn Calculations," DASA-1528 (E. H. Plesset Assoc., Inc., Report 56321), June 24, 1964. Also Mayer and Richey, J. Opt. Soc. Amer. 54, 678 (1964).
4. Glenn A. Fry, Blur of the Retinal Image (Ohio State Univ. Press, Columbus, 1955), Chap. 9.
5. F. Flamant, Rev. Optique 34, 433 (1955).
6. K. N. Ogle, J. Opt. Soc. Amer. 52, 1035 (1962).
7. G. Westheimer and F. W. Campbell, J. Opt. Soc. Amer. 52, 1040 (1962).
8. J. Krauskopf, J. Opt. Soc. Amer. 52, 1046 (1962).
9. J. Krauskopf, J. Opt. Soc. Amer. 54, 715 (1964).
10. E. W. Marchand, J. Opt. Soc. Amer. 54, 915 (1964).
11. Alfred Cowan, Refraction of the Eye (Lea and Febiger, Philadelphia, 1948), p. 125.
12. W. S. Spector, ed., Handbook of Biological Data (W. B. Saunders, Philadelphia, 1956), p. 316. (Also available as report WADC-TR-56-273.)
13. C. Curry, Geometrical Optics (Edward Arnold and Co., London, 1953), Chap. IV.
14. M. Born and E. Wolf, Principles of Optics (Pergamon Press, New York

City, 2nd ed., 1964), pp. 395-398.

15. H. Helmholtz, Treatise on Physiological Optics (orig. publ. 1856; transl. from 3rd German ed. publ. by Opt. Soc. Amer., Rochester, N.Y., 1924), vol. I, pp. 172 ff.

16. E. A. Boettner and J. R. Wolter, MRL-TDR-62-34 (May, 1962).

17. N. I. Pinegin, Comptes Rendus Acad. Sci. URSS 30, 206 (1941).

18. G. Wald and D. R. Griffin, J. Opt. Soc. Amer. 37, 321 (1947).

19. R. E. Bedford and G. Wyszecki, J. Opt. Soc. Amer. 47, 564 (1957).

20. K. Mütze, Optik 14, 97 (1957).

21. John Taylor, reported in reference 3.

22. A. Linksz, Physiology of the Eye (Grune and Stratton, New York, 1950), vol. I (Optics), Chap. 17, esp. Figs. 134-5 and Table I.

23. W. S. Duke-Elder, Text-Book of Ophthalmology (C. V. Mosby Co., St. Louis, 1949), vol. IV, Chap. LI.

24. M. Françon, M. Cagnet, and J. C. Thrierr, Atlas of Optical Phenomena (Prentice-Hall, Englewood Cliffs, N.J., 1962), plates 16, 21, 23.

25. E. Lommel, Abh. Bayer. Akad. 15, pt. 2, 233 (1885).

26. Reference 14, pp. 435-445.

27. H. H. Hopkins, Proc. Phys. Soc. (London) B62, 22 (1949).

28. E. Wolff, Anatomy of the Eye and Orbit (Blakiston Co., New York City, 4th ed. 1954), pp. 421 ff.

29. C. Berens, ed., The Eye and Its Diseases (W. B. Saunders and Co., Philadelphia, 2nd ed., 1949), p. 36.

30. Reference 12, p. 317; S. G. de Groot and J. W. Gebhard, J. Opt. Soc.

Amer. 42, 492 (1952); R. Leinhos, Optik 16, 669 (1959).

31. American Institute of Physics Handbook (McGraw-Hill Book Co., New York, 1963), 2nd ed., Tables 6d-2 and 6e-1.

32. M. Koomen, R. Tousey, and R. Scolnik, J. Opt. Soc. Amer. 39, 370 (1949); 46, 903 (1956). A. Ivanoff, J. Opt. Soc. Amer. 46, 901 (1956).

33. Reference 14, p. 204.

34. M. S. Smirnov, Biofizika (Engl. transl.) 6, 776 (1961).

35. Reference 14, Chap. IX.

36. D. W. DeMott and R. M. Boynton, J. Opt. Soc. Amer. 48, 13 (1958).

37. R. M. Boynton and F. J. J. Clarke, J. Opt. Soc. Amer. 54, 110, 1170 (1964).

38. J. J. Vos and M. A. Bouman, J. Opt. Soc. Amer. 54, 95 (1964).

39. Reference 28, Chaps. II and IV.

40. R. D. Cowan, et al., LAMS-2749 (Sept. 14, 1962). (Classified report.)

41. W. T. Ham, Jr., R. C. Williams, W. J. Geeraets, R. S. Ruffin, and H. A. Mueller, Acta Ophthalmologica, Supp. 76, 60 (1963).

42. W. T. Ham, Jr., et al., J. Opt. Soc. Amer. 54, 566 (1964) -- details to be published.

43. Reference 31, Table 6k-11.